State Stabilization in Open Quantum Systems

BY

DAVID CAMPBELL

ABSTRACT OF A THESIS SUBMITTED TO THE FACULTY OF THE
DEPARTMENT OF PHYSICS AND APPLIED PHYSICS
IN PARTIAL FULFILLMENT OF THE REQUIREMENTS
FOR THE DEGREE OF
MASTER OF SCIENCE UNIVERSITY OF MASSACHUSETTS LOWELL
2019

Thesis Supervisor: Archana Kamal, Ph.D.
Assistant Professor, Department of Physics and Applied Physics

State Stabilization in Open Quantum Systems

BY

DAVID CAMPBELL
B.S. UNIVERSITY OF MASSACHUSETTS LOWELL (2016)

SUBMITTED IN PARTIAL FULFILLMENT OF THE REQUIREMENTS
FOR THE DEGREE OF MASTER OF SCIENCE
DEPARTMENT OF PHYSICS AND APPLIED PHYSICS
UNIVERSITY OF MASSACHUSETTS LOWELL

Signature of Author: David Campbell **Date:** 5/4/2019

Signature of Thesis Committee Chair:

Prof. Archana Kamal: Archana Kamal

Signatures of Thesis Committee Members:

Prof. Viktor Podolskiy:

Prof. Nishant Agarwal:

Prof. Jayant Kumar: Jkumar

Abstract

Quantum state engineering and control is a mainstay of any quantum information platform. The primary roadblock in preserving quantum states is the phenomenon of decoherence, which washes out quantum coherences due to inevitable coupling of quantum systems with uncontrolled degrees of freedom. For many years, the strategy behind fighting decoherence primarily relied on coming up with ways to isolate the quantum state (or system) of interest from the surrounding environment. In recent years, however, there has been a push to use dissipation as a resource instead, and wield it as an alternative to Hamiltonian engineering for controlling quantum dynamics. This view is justified by the ability to "engineer" system-environment couplings such that the effective dissipation seen by the quantum system is modified.

In this thesis, we analyze dissipation engineering protocols that can stabilize entangled states of two or more qubits. The particular theoretical procedure employed to determine the engineered dissipation seen by the qubit system is adiabatic elimination, which is applicable when the environment degrees of freedom evolve on time scales much faster than those relevant for the system subspace. We use this formalism to calculate the fidelity and rate of stabilization of a Bell state, where the two qubits (a.k.a. Alice and Bob) are coupled purely via dissipation. We extend our studies to the case when combining such a dissipative interaction with a coherent qubit-qubit interaction renders the coupling between qubits directional. We show how such directionality is crucial to realize multipartite entanglement using a system of four qubits. Our studies are directly relevant to the widely-used paradigm of cavity- and circuit-

quantum electrodynamics and can be extended to study entanglement dynamics in larger quantum networks.

Acknowledgments

First I would like to thank my advisor Prof. Archana Kamal for her support, encouragement, assistance, and patience when guiding me through this project. I would like to extend a special thanks to Prof. Nishant Argarwal for his assistance and guidance on side projects that help inspire this work. To my committee members, Prof. Viktor Podolskiy, and Prof. Jayant Kumar, thank you for your mentorship over the past couple years.

I would like to extend gratitude to my group members who collaborated with me on my research. They include, in no particular order, Alvin Kow, Emery Doucet, and Tristan Brown. I have had many insightful conversations with them.

Finally, I would like to thank my parents for their support on this journey. Also for their patience/attention they gave me when I explained my work to them.

Contents

List of Tables

List of Figures

Chapter 1

Introduction

At its core quantum computation combines two of the biggest scientific and technological breakthroughs of the last century: the first being quantum mechanics with its strange and counter-intuitive interpretations, and the second being integrated logic circuits which gave rise to digital computers and fueled the information age. The central tenet of quantum information processing is to replace the classical bits that are either '1' OR '0', with quantum bits ("qubits") that can be in a coherent superposition of '1' AND '0'. However, the practical challenge of preserving these superpositions is daunting. This is because quantum systems typically couple to uncontrolled degrees of freedom in their environment that cause them to decay into classical mixtures [2]. This poses the primary challenges for quantum engineers today – namely decoherence, or the phenomenon that destroys quantum information due to parasitic coupling of qubits to uncontrolled environmental degrees of freedom. Traditionally the efforts to mitigate decoherence have focused on eliminated or minimizing such unwanted interactions. However, it has recently been shown that system-environment couplings can be "engineered" in a manner that allows us to use dissipation to our advantage. In particular, the system can be driven into a pure state state by the dissipation, if the environment serves as a Maxwell demon and evacuates entropy from the quantum system of interest [3]. Such an approach has even been extended to stabilize

multi-particle states known as matrix-product states. [4–6].

Use of dissipation engineering to stabilize entangled states has recently gained a lot of theoretical and experimental attention. This is because entanglement is important to many quantum information applications. One example is quantum teleportation, a process by which quantum information can be transmitted from one location to another over a classical communication channel if the sender and receiver share an entangled pair of qubits. Entangled states also form the basis of quantum cryptography and quantum error correction protocols. However, such states are particularly sensitive to deocherence since local noise seen by any of the qubits forming the entangled state can destroy the quantum information encoded in non-local correlations. Thus preserving entanglement for long times is a simultaneously a challenging and compelling prospect. In this thesis, we specifically focus on dissipative stabilization of two- and four-qubit entangled states with high-fidelity.

This thesis is organized as follows: in chapter 2, we introduce open quantum system formalism and present the derivation of quantum master equation that captures the influence of the environment on a quantum system. Using the master equation to describe a single qubit coupled to a radiation field at finite temperature, we show how dissipation into the environment leads to decoherence. In chapter 3, we introduce the notion of dark states that are the pure steady states of an open system. We detail the method of adiabatic elimination which allows identification of dark state of an open system, and use it to study stabilization of a Bell state in a system of two qubits coupled to the fundamental mode of a resonator (described using a simple harmonic oscillator). We compare our results for fidelity and rate of Bell state stabilization for the cases when flow of excitations in the two-qubit subsystem is bidirectional (symmetric) vs unidirectional (chiral). In chapter 4, we extend our scheme to four-qubits and show how purification of multipartite entanglement can be achieved in this framework. Chapter 5 presents a brief summary of our results and potential extensions for future studies.

Chapter 2

Open Quantum Systems

In general it is impossible to prevent any quantum system, such as an atom/molecule or superconducting qubit, from coupling to its surroundings or the environment [7]. This leads to phenomenon of decoherence which represents loss of information from a system to its environment. Since the environment typically consists of a several degrees of freedom that we are unable to track or control, either experimentally or theoretically, the coherence is usually irretrievably lost. Due to decoherence the usual steady state of the system is a statistical mixture. Such a mixture necessitates the description of the system via a density matrix instead of the usual state vector describing a wavefunction. The formalism of open quantum systems (OQS) is employed to study the behavior of such systems of interest interacting with extraneous degrees of freedom. The typical OQS methods partition the full Hilbert space into a system space S (atom/qubit), and a reservoir space R (representing the environment). Since we are only interested in the dynamical behavior of degrees of freedom that belong to the system S, the reservoir degrees of freedom, R, are ultimately traced over; a procedure called partial trace. Figure 2.1 gives a schematic description of this procedure, where the ultimate goal is to get a dynamical map $V(t)$ describing the evolution of the reduced system.

In the following sections, we present a detailed derivation of a widely used form

$$\begin{array}{ccc} \chi(0) = \rho_{\mathcal{S}}(0) \otimes \rho_{\mathcal{R}}(0) & \xrightarrow{\text{Unitary Evolution}} & \chi(t) = \hat{U}(t)\left(\rho_{\mathcal{S}}(0) \otimes \rho_{\mathcal{R}}(0)\right)\hat{U}(t) \\ \downarrow tr_{\mathcal{R}} & & \downarrow tr_{\mathcal{R}} \\ \rho_{\mathcal{S}}(0) & \xrightarrow{\text{Dynamical Map}} & \rho_{\mathcal{S}}(t) = V(t)\rho_{\mathcal{S}}(0) \end{array}$$

Figure 2.1: Two potential ways of partial trace over the environment. Here $\chi(0)$ represents the full density operator of system and reservoir, while ρ_S describes the density operator of the reduced system.

of this dynamical map relevant for 'weak' system-reservoir coupling (perturbative regime), that leads to an equation of motion for the reduced system called Gorini–Kossakowski– Sudarshan– Lindblad (GKSL) equation. As a means of demonstration, we use this to describe a single qubit weakly coupled to an environment, consisting of a collection of independent oscillators, and derive optical Bloch equations describing the dynamics of a driven-dissipative qubit.

2.1 Quantum Master (GKSL) Equation

Let us consider the Liouville-von Neumann equation in the Schrödinger picture

$$\dot{\chi} = -\frac{i}{\hbar}[H, \chi], \tag{2.1.1}$$

which captures the time dynamics of the density operator

$$\chi = \sum_n p_n \left|\Psi_n\right\rangle \left\langle\Psi_n\right| \tag{2.1.2}$$

for both the system and the reservoir, $S + R$. Partitioning the Hilbert space into system and reservoir subspace, the Hamiltonian can be written as

$$H = H_{\mathcal{S}} \otimes I_{\mathcal{R}} + I_{\mathcal{S}} \otimes H_{\mathcal{R}} + H_{\mathcal{SR}} \tag{2.1.3}$$

where $H_{\mathcal{S}} \in \mathcal{H}_{\mathcal{S}}$, $H_{\mathcal{R}} \in \mathcal{H}_{\mathcal{R}}$, and $H_{\mathcal{SR}} \in \mathcal{H}$ mediates the interaction between the the two subspaces (Fig. 2.2). Typically, the tensor products with the complement space are assumed, and will be henceforth suppressed for brevity of notation. To zoom in

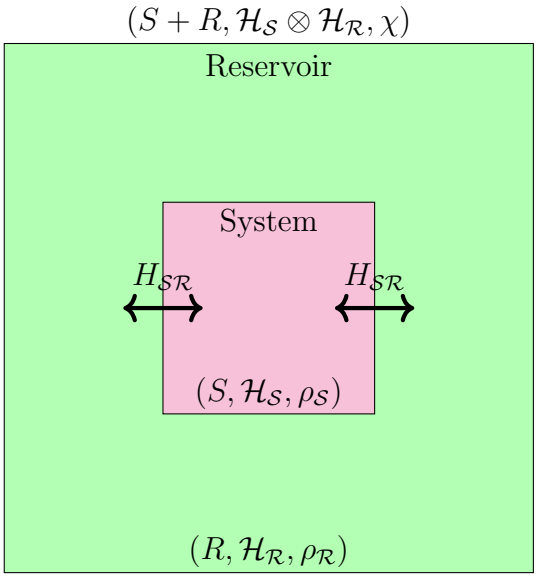

Figure 2.2: Partitioning of the full Hilbert space into system and reservoir subspaces.

on the slow dynamics caused by the interaction $H_{\mathcal{SR}}$, we move into the interaction picture. Defining

$$\tilde{\chi}(t) = e^{i(H_\mathcal{S}+H_\mathcal{R})t/\hbar}\chi e^{-i(H_\mathcal{S}+H_\mathcal{R})t/\hbar} \tag{2.1.4}$$

and taking the time derivative of Eq. (2.1.4), we obtain

$$\begin{aligned}\dot{\tilde{\chi}} &= \frac{i}{\hbar}(H_\mathcal{R}+H_\mathcal{S})\tilde{\chi} - \frac{i}{\hbar}\tilde{\chi}(H_\mathcal{R}+H_\mathcal{S}) + e^{i(H_\mathcal{S}+H_\mathcal{R})t/\hbar}\dot{\chi}e^{-i(H_\mathcal{S}+H_\mathcal{R})t/\hbar} \\ &= -\frac{i}{\hbar}[\tilde{H}_{\mathcal{SR}}(t), \tilde{\chi}(t)],\end{aligned} \tag{2.1.5}$$

where

$$\tilde{H}_{\mathcal{SR}}(t) = e^{i(H_\mathcal{S}+H_\mathcal{R})t/\hbar}H_{\mathcal{SR}}e^{-i(H_\mathcal{S}+H_\mathcal{R})t/\hbar}. \tag{2.1.6}$$

The formal solution to this equation is

$$\tilde{\chi}(t) = \chi(0) - \frac{i}{\hbar}\int_0^t ds\,[\tilde{H}_{\mathcal{SR}}(s), \tilde{\chi}(s)]. \tag{2.1.7}$$

Note that $\tilde{\chi}(0) = \chi(0)$. Substituting the formal solution, Eq. (2.1.7), in Eq. (2.1.5), we obtain the equation for the full density operator in the interaction picture

$$\dot{\tilde{\chi}} = -\frac{i}{\hbar}[\tilde{H}_{\mathcal{SR}}(t), \chi(0)] - \frac{1}{\hbar^2}\int_0^t ds\,[\tilde{H}_{\mathcal{SR}}(t), [\tilde{H}_{\mathcal{SR}}(s), \tilde{\chi}(s)]]. \tag{2.1.8}$$

In order to obtain an equation describing dynamics of the reduced system, S, we partial trace over the reservoir degrees of freedom

$$\dot{\tilde{\rho}} = -\frac{1}{\hbar^2}\int_0^t ds\, tr_{\mathcal{R}}\left\{[\tilde{H}_{\mathcal{SR}}(t),[\tilde{H}_{\mathcal{SR}}(s),\tilde{\chi}(s)]]\right\}. \tag{2.1.9}$$

Here, $\tilde{\rho}_{\mathcal{S}}(t) = tr_{\mathcal{R}}\{\tilde{\chi}(t)\}$ and we assumed that

$$tr_{\mathcal{R}}\left\{[\tilde{H}_{\mathcal{SR}}(t),\chi(0)]\right\} = 0. \tag{2.1.10}$$

The assumption is true when the reservoir is in the vacuum state; for any general state of the reservoir this can be ensured by adding the term $tr_{\mathcal{R}}\{H_{\mathcal{SR}}\rho_{\mathcal{R}}\}$ to the system Hamiltonian [8]. At this stage Eq. (2.1.9) is exact since no approximations have been made so far.

2.1.1 Born-Markov Approximation

The first assumption that is made is the system and reservoir begin uncorrelated and remain uncorrelated because $H_{\mathcal{SR}}$ is weak. Furthermore, it is assumed that density operator of the environment is time-independent. This implies,

$$\tilde{\chi}(t) = \tilde{\rho}_{\mathcal{S}}(t)\otimes\rho_{\mathcal{R}}. \tag{2.1.11}$$

so

$$\dot{\tilde{\rho}}_{\mathcal{S}} = -\frac{1}{\hbar^2}\int_0^t ds\, tr_{\mathcal{R}}\left\{[\tilde{H}_I(t),[\tilde{H}_I(s),\tilde{\rho}_{\mathcal{S}}(s)\otimes\rho_{\mathcal{R}}]]\right\}. \tag{2.1.12}$$

Typically correlations (entanglement) between the subsystems build up because of the interaction. Thus we are assuming the reservoir is so large, compared to the system, that it is virtually unaffected by the coupling to the system. This equation is sometimes called the Redfield equation which was developed in the context of nuclear magnetic resonance [9].

To proceed any further, we have to be more specific about the form of the interaction. Since the interaction acts on both subspaces, without loss of generality, we

can decompose the interaction as

$$H_{\mathcal{SR}} = \hbar \sum_{\alpha} A_{\alpha} \otimes b_{\alpha}^{\dagger} + h.c. \tag{2.1.13}$$

where $b_{\alpha}^{\dagger}$ denotes the creation operator for a given oscillator comprising the reservoir. Then moving into the interaction picture, this gives

$$\tilde{H}_{\mathcal{SR}}(t) = \hbar \sum_{\alpha} A_{\alpha}(t) \otimes b_{\alpha}^{\dagger}(t) + h.c. \tag{2.1.14}$$

where $A_{\alpha}(t) = e^{iH_{\mathcal{S}}t/\hbar} A_{\alpha} e^{-iH_{\mathcal{S}}t/\hbar}$ and $b_{\alpha}(t) = e^{iH_{\mathcal{R}}t/\hbar} b_{\alpha} e^{-iH_{\mathcal{R}}t/\hbar}$. For a reservoir in a thermal state at temperature T, the density operator can be written as,

$$\rho_{\mathcal{R}} = \frac{1}{tr_{\mathcal{R}}\{e^{-H_{\mathcal{R}}/kT}\}} e^{-H_{\mathcal{R}}/kT}. \tag{2.1.15}$$

where $H_{\mathcal{R}} = \hbar \sum_{\alpha} \omega_{\alpha} b_{\alpha}^{\dagger} b_{\alpha}$. We are now able to trace over the reservoir degrees of freedom

$$\begin{aligned} \dot{\tilde{\rho}}_{\mathcal{S}} = \sum_{\alpha\beta} \int_0^t d\tau \Big\{ & \left[A_{\beta}(t-\tau)\tilde{\rho}_{\mathcal{S}}, A_{\alpha}(t) \right] \left\langle b_{\alpha}(t) b_{\beta}(t-\tau) \right\rangle \\ & + \left[A_{\beta}^{\dagger}(t-\tau)\tilde{\rho}_{\mathcal{S}}, A_{\alpha}^{\dagger}(t) \right] \left\langle b_{\alpha}^{\dagger}(t) b_{\beta}^{\dagger}(t-\tau) \right\rangle \\ & + \left[A_{\beta}^{\dagger}(t-\tau)\tilde{\rho}_{\mathcal{S}}, A_{\alpha}(t) \right] \left\langle b_{\alpha}(t) b_{\beta}^{\dagger}(t-\tau) \right\rangle \\ & + \left[A_{\beta}(t-\tau)\tilde{\rho}_{\mathcal{S}}, A_{\alpha}^{\dagger}(t) \right] \left\langle b_{\alpha}^{\dagger}(t) b_{\beta}(t-\tau) \right\rangle + h.c. \Big\} \end{aligned} \tag{2.1.16}$$

To proceed any further we need to evaluate the correlation functions of the reservoir. For a Markovian reservoir, these correlation functions decay more rapidly than any timescale associated with the system. Ideally, they would decay instantaneously i.e. [8]

$$\left\langle b_{\alpha}^{\dagger}(t) b_{\beta}(s) \right\rangle \sim \delta(t-s). \tag{2.1.17}$$

Calculating the correlation functions explicitly, we find

$$\left\langle b_{\alpha}(t) b_{\beta}(t-\tau) \right\rangle = \left\langle b_{\alpha}^{\dagger}(t) b_{\beta}^{\dagger}(t-\tau) \right\rangle = 0 \tag{2.1.18}$$

$$\left\langle b_{\alpha}^{\dagger}(t) b_{\beta}(t-\tau) \right\rangle = \gamma_{\alpha} N(\omega_{\alpha}) \delta_{\alpha\beta} \delta(\tau) \tag{2.1.19}$$

$$\left\langle b_{\alpha}(t) b_{\beta}^{\dagger}(t-\tau) \right\rangle = \gamma_{\alpha} (1 + N(\omega_{\alpha})) \delta_{\alpha\beta} \delta(\tau) \tag{2.1.20}$$

where

$$N_{\omega\alpha} = \frac{1}{e^{\hbar\omega_\alpha/k_BT} - 1} \tag{2.1.21}$$

is the Bose-Einstein occupation number. Substituting the correlation functions in Eq. (2.1.16), we obtain

$$\dot{\tilde{\rho}}_{\mathcal{S}} = \sum_\alpha \gamma_\alpha \left\{ \left[A_\alpha^\dagger(t)\tilde{\rho}_{\mathcal{S}}, A_\alpha(t)\right] (1 + N(\omega_\alpha)) + \left[A_\alpha(t)\tilde{\rho}_{\mathcal{S}}, A_\alpha^\dagger(t)\right] N(\omega_\alpha) + h.c. \right\}$$

Moving back into the Schrodinger picture using

$$\dot{\rho}_{\mathcal{S}} = -\frac{i}{\hbar}[H_{\mathcal{S}}, \rho_{\mathcal{S}}] + e^{-iH_{\mathcal{S}}t} \left(\frac{d}{dt}\dot{\tilde{\rho}}_{\mathcal{S}}\right) e^{iH_{\mathcal{S}}t} \tag{2.1.22}$$

we find

$$\dot{\rho}_{\mathcal{S}} = -\frac{i}{\hbar}[H_{\mathcal{S}}, \rho_{\mathcal{S}}] + \sum_\alpha \gamma_\alpha \left\{ \left[A_\alpha^\dagger \rho_{\mathcal{S}}, A_\alpha\right] (1 + N(\omega_\alpha)) + \left[A_\alpha \rho_{\mathcal{S}}, A_\alpha^\dagger\right] N(\omega_\alpha) + h.c. \right\}.$$

Expanding out the commutators we can write

$$\begin{aligned} \dot{\rho}_{\mathcal{S}} = &-\frac{i}{\hbar}[H_{\mathcal{S}}, \rho_{\mathcal{S}}] \\ &+ \sum_\alpha \frac{\gamma_\alpha}{2} \left[(1 + N_{\omega_\alpha}) \left(A_\alpha \rho_{\mathcal{S}} A_\alpha^\dagger + \frac{1}{2}\left\{A_\alpha^\dagger A_\alpha, \rho_{\mathcal{S}}\right\} \right) \right. \\ &\left. + N_{\omega_\alpha} \left(A_\alpha^\dagger \rho_{\mathcal{S}} A_\alpha + \frac{1}{2}\left\{A_\alpha A_\alpha^\dagger, \rho_{\mathcal{S}}\right\} \right) \right]. \end{aligned} \tag{2.1.23}$$

We now have have an equation that captures the effective dynamics of the open system $\mathcal{S}$. Typically, A_α is proportional to a lowering operator. This makes the second term describe decay of the system into the reservoir, with a rate proportional $\gamma_\alpha(1 + N_{\omega_k})$. And the third term proportional to absorption of the system from the reservoir.

2.2 Optical Bloch Equations

We now present a simple example of a driven-dissipative two-level system (a.k.a. qubit), coupled to a reservoir, with an XX-type interaction. The total Hamiltonian

is is the sum $H = H_{\mathcal{S}} + H_{\mathcal{R}} + H_{\mathcal{SR}}$, where

$$\begin{aligned} H_{\mathcal{R}} &= \omega_c b^\dagger b \\ H_{\mathcal{S}} &= \frac{\epsilon}{2}\sigma_z + \Omega\cos(\omega_l t)\sigma_x \\ H_{\mathcal{SR}} &= g\sigma_x \sum_\alpha \left(b_\alpha + b_\alpha^\dagger\right). \end{aligned} \tag{2.2.1}$$

To avoid the fast dynamics caused by the drive we move into a rotating frame (RF) with a unitary

$$U = exp\left(-i\left\{\sum_\alpha \omega_\alpha b_\alpha^\dagger b_\alpha + \frac{\omega_l}{2}\sigma_z\right\}\right) \tag{2.2.2}$$

This transforms $b_\alpha \to b_\alpha e^{-i\omega_\alpha t}$ and $\sigma \to \sigma e^{-i\omega_l t}$ thus modifying the different pieces of the Hamiltonian as (see Appendix A),

$$\begin{aligned} H'_{\mathcal{R}} &= 0 \\ H'_{\mathcal{S}} &\approx \frac{\delta}{2}\sigma_z + \frac{\Omega}{2}(e^{i\omega_l t} + e^{-i\omega_l t})(\sigma e^{-i\omega_l t} + \sigma^\dagger e^{i\omega_l t}) \\ H'_{\mathcal{SR}} &= g\sum_\alpha (b_\alpha e^{-i\omega_\alpha t} + b^\dagger e^{i\omega_\alpha t})(\sigma e^{-i\omega_l t} + \sigma^\dagger e^{i\omega_l t}), \end{aligned} \tag{2.2.3}$$

where we have expressed cosine function in terms of exponential. The symbol $\delta = \epsilon - \omega_l$ denotes the detuning of qubit resonant frequency and the drive frequency system. Ignoring fast oscillating terms under a rotating wave approximation (RWA) [10], the resultant Hamiltonian is

$$\begin{aligned} H'_{\mathcal{S}} &\approx \frac{\delta}{2}\sigma_z + \frac{\Omega}{2}\sigma_x \\ H'_{\mathcal{SR}} &\approx g\sum_\alpha (\sigma b_\alpha^\dagger e^{-i\Delta t} + h.c.), \end{aligned} \tag{2.2.4}$$

where $\Delta = \omega_l - \omega_\alpha$. The interaction in Eq. (2.2.4) is often called the Jaynes-Cummings interaction. Comparing it to Eq.(2.1.13) and identifying $A_\alpha = \sigma$. Substituting into Eq. (2.1.23), we can write the master equation for this driven-dissipative qubit as

$$\begin{aligned} \dot{\rho}_{\mathcal{S}} = &-i\frac{\delta}{2}[\sigma_z, \rho] - i\frac{\Omega}{2}[\sigma_x, \rho] \\ &+ \gamma(1 + N_{\omega_b})\left(\sigma\rho_{\mathcal{S}}\sigma^\dagger - \frac{1}{2}\left\{\sigma^\dagger\sigma, \rho_{\mathcal{S}}\right\}\right) + \gamma N_{\omega_b}\left(\sigma^\dagger\rho_{\mathcal{S}}\sigma - \frac{1}{2}\left\{\sigma\sigma^\dagger, \rho_{\mathcal{S}}\right\}\right), \end{aligned} \tag{2.2.5}$$

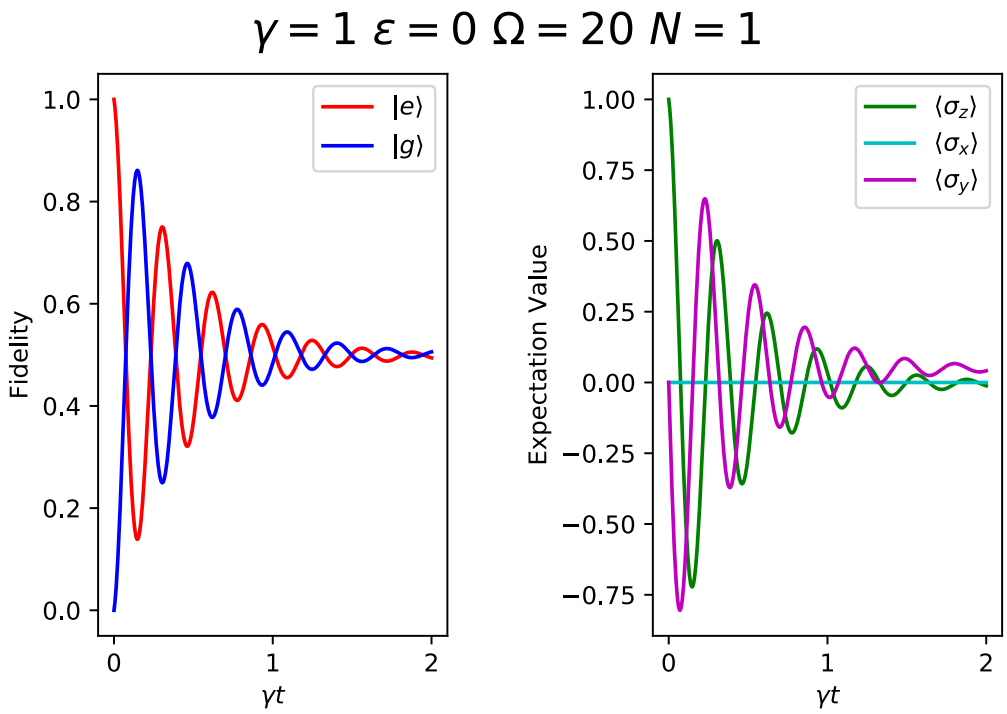

Figure 2.3: (Left Panel) Numerical simulation of optical Bloch equations showing a decay of Rabi oscillations. (Right panel) Furthermore, the expectation values of all the Pauli operators are decaying towards zero which means that the steady state of qubit is a mixed state. Since excitations leave and enter the system stochastically (i.e. not coherently) its not surprising the state has decohered [1].

with $N_{\omega_b} = Tr\{\rho_B b^\dagger b\}$. In writing this equation, we have assumed $(\omega_\alpha - \omega_l) \ll \tau_{\mathcal{R}}^{-1}$, where $\tau_{\mathcal{R}}$ is the relaxation time of the reservoir [11]. The second term in this equation is responsible for decay into the reservoir, at a rate $\gamma(1 + N_{\omega_b})$. This rate captures both simulated emission that scales with bath occupation number (i.e. γN_{ω_b}) and spontaneous emission γ corresponding to decay induced due to vacuum fluctuations. The third term is responsible for absorption into the system at a rate γN_{ω_b}.

The expectation values for the Pauli operators are

$$\begin{aligned}
\langle \dot{\sigma}_x \rangle &= -\gamma \left(2N_{\omega_b}+1\right)\langle \sigma_x \rangle - \delta \langle \sigma_y \rangle \\
\langle \dot{\sigma}_y \rangle &= \delta \langle \sigma_x \rangle - \gamma \left(2N_{\omega_b}+1\right) - \Omega \langle \sigma_z \rangle \\
\langle \dot{\sigma}_z \rangle &= \Omega \langle \sigma_y \rangle - 2\gamma[\langle \sigma_z \rangle \left(2N_{\omega_b}+1\right)+1].
\end{aligned} \tag{2.2.6}$$

They are called optical Bloch equations. Numerical simulations in Fig. 2.3 show that the expectation values of Pauli operators decay to zero.

The steady state density matrix of Eq. (2.2.5) was found to be

$$\rho_S \xrightarrow{t\to\infty} \frac{1}{2}\left(|e\rangle\langle e| + |g\rangle\langle g|\right), \tag{2.2.7}$$

which is referred to as a mixed state, and is distinguished from a coherent superposition,

$$|\Psi\rangle_S = \frac{1}{\sqrt{2}}\left(|e\rangle + e^{i\phi}|g\rangle\right), \tag{2.2.8}$$

which we called a pure state. Though the probabilities of being found in the excited or ground state are same for both the pure and mixed state, their origins are quite different. The probabilities associated with Eq. (2.2.7) arise from the uncertainty in the state of the system. This is in contrast with Eq. (2.2.8) where the state can be represented with a well-defined ket in $\mathcal{H}_S$. The probabilities of 1/2 obtained from measurement of such a superposition are intrinsic to quantum mechanics, and not necessarily due to ignorance or uncertainty about the state of the system as is the case for a statistical mixture.

Another way to see this is that there is a fixed phase relationship between the states $|e\rangle$ and $|g\rangle$ in Eq. (2.2.8) that contains vital information about its orientation on the Bloch sphere. There is no phase relation between the excited and ground state in Eq. (2.2.7) however. This evolution of a state into a statistical mixture, resulting in the loss of encoded coherent information, is referred to as decoherence.

Chapter 3

Bell State Stabilization

As evident from the results presented in last chapter, dissipation destroys quantum coherences leading to steady states that are statistical mixtures of classical states. In this chapter, we will show how dissipation seen by the quantum systems can be engineered such that the system settles into a pure quantum state. Specifically, since Bell states are important to quantum information platforms, we will present a protocol where the steady state of dissipation-driven two-qubit system is

$$\rho \xrightarrow{t\to\infty} |\Phi\rangle \langle\Phi| , \tag{3.0.1}$$

where $|\Phi\rangle = (|eg\rangle - |ge\rangle)/\sqrt{2}$ is a maximally entangled singlet state.

We will first introduce the Liouvillian superoperator that describes the evolution of an open quantum system (analogous to the Hamiltonian describing the evolution of a closed quantum system). This description will allow us to introduce the notions of fidelity and gap for a stabilization protocol. We will then describe the conditions that need to be satisfied for a dissipative process to have a pure steady state — in particular, we detail the method of adiabatic elimination that allows to eliminate bath modes constituting a fast subspace of the problem and write engineered dissipators seen by the reduced quantum system of interest. We will then use this method to analyze a system of two qubits coupled to a lossy resonator. We will consider two specific cases:

- *Symmetric Case*: In this case the two qubits effectively "talk" to each other through the resonator mode, which manifests itself as an effective dissipative interaction between the qubits once the resonator mode is eliminated.

- *Chiral Case*: In this we will add a direct coherent interaction between the qubits, and tune the relative phase between the dissipative and coherent interactions such that one qubit "sees" the other but not vice-versa.

3.1 Liouvillian

In essence, the quantum master (GKSL) equation introduced in the previous chapter is the Liouville-von Neumann equation plus a dissipator, defined as

$$\mathcal{D}[c_l]\rho = \left(c_l \rho c_l^\dagger - \frac{1}{2} \left\{ c_l^\dagger c_l, \rho \right\} \right) \tag{3.1.1}$$

The dissipator is a function of a quantum jump operator, c_l, that captures the "engineered" decay/absorption process with an associated rate $\gamma_l \geq 0$. Whether the dissipator is associated with decay/absorption into the reservoir depends if the collapse operator is proportional to a creation or annihilation operator. Here we rewrite the quantum master equation as an eigenvalue equation

$$\dot{\rho} = \mathcal{L}\rho \tag{3.1.2}$$

by defining the Liouvillian superoperator as

$$\mathcal{L}\bullet = -\frac{i}{\hbar}[H, \bullet] + \sum_n \gamma_l \left(c_l \bullet c_l^\dagger - \frac{1}{2} \left\{ c_l^\dagger c_l, \bullet \right\} \right). \tag{3.1.3}$$

Using the above notation, we can write the formal solution to GKSL equation as

$$\rho(t) = e^{\mathcal{L}t}\rho(0). \tag{3.1.4}$$

Note that this assumes that the Hamiltonian and jump operators are time-independent.

Converting the Liouvillian superoperator, $\mathcal{L}\bullet$, converted into an $n^2 \times n^2$ matrix, L, and the density matrix, ρ, into a $n^2 \times 1$ column vector we write the formal solution 3.1.4 in terms of the eigenvalues of L.

$$\vec{\rho}(t) = e^{\mathcal{L}t}\vec{\rho} = \sum_n e^{\lambda_n}\vec{\rho}_n \tag{3.1.5}$$

For simplicity we are assuming non-degeneracy. It turns out the Liouvillian matrix has a single zero eigenvalue with the rest coming in conjugate pairs with a negative real part. The eigenvector corresponding to zero is the steady state, ρ_{ss}, because $\rho \xrightarrow{t\to\infty} \rho_{ss}$. The speed at which a system approaches ρ_{ss} is called the gap, $\Delta_{\mathcal{L}}$, and is equal to the eigenvalue with the smallest real part [12]. How "close" the steady state is to a bell state, $|\Phi\rangle$. The metric of this "closeness" is called the fidelity and is defined as

$$F_{|\Phi\rangle} = tr\{|\Phi\rangle\langle\Phi|\rho_{ss}\}. \tag{3.1.6}$$

3.2 Dark States

We rewrite the Liouvillian in terms of the positive map, $\mathcal{E}(\rho) = 2\sum_l \gamma_l c_l \rho c_l^\dagger$, and $Q = P - iH$, with $P = \sum_l \gamma_l c_l^\dagger c_l$ [12].

$$\mathcal{L}\rho = \mathcal{E}(\rho) - Q^\dagger\rho - \rho Q \tag{3.2.1}$$

Theorem 1. *Let $\mathcal{L}$ be defined as in Eq. (3.2.1). Then $\mathcal{L}(|\Phi\rangle\langle\Phi|) = 0$ if and only if the following two conditions are satisfied:*

(1) $Q^\dagger|\Phi\rangle = \lambda|\Phi\rangle$ for some $\lambda \in \mathbb{C}$

(2) $c_l|\Phi\rangle = \lambda_l|\Phi\rangle$ for some $\lambda_l \in \mathbb{C}$ with $\sum_l g_l|\lambda_l|^2 = Re(\lambda)$.

Proof. If $\mathcal{L}(|\Phi\rangle\langle\Phi|) = 0$ then

$$\begin{aligned} \mathcal{E}(|\Phi\rangle\langle\Phi|) &= Q^\dagger|\Phi\rangle\langle\Phi| + |\Phi\rangle\langle\Phi|Q \\ 2\sum_l g_l|\Psi_l\rangle\langle\Psi_l| &= |\Phi\rangle\langle\eta| + |\eta\rangle\langle\Phi| \end{aligned} \tag{3.2.2}$$

with $|\Psi_l\rangle = c_l |\Phi\rangle$ and $Q^\dagger |\Phi\rangle = |\chi\rangle$. Since the left-hand-side of Eq. (3.2.2) is a positive operator (ie. $g_l \geq 0$), the right-hand-side must also be a positive operator. However, the right-hand-side is a Pauli σ_x operator in bra-ket notation which has a negative eigenvalue, a contradiction. It can be shown that $A = |\Phi\rangle\langle\eta| + |\eta\rangle\langle\Phi|$ is positive if and only if its rank is one, that is $|\chi\rangle = \lambda |\Phi\rangle$ for some $\lambda \in \mathbb{C}$

$$Q^\dagger |\Phi\rangle = |\chi\rangle = \lambda |\Phi\rangle . \tag{3.2.3}$$

Thus condition *(1)* is satisfied. Rewriting Eq. (3.2.2)

$$2\sum_l g_l |\Psi_l\rangle\langle\Psi_l| = 2\,\mathrm{Re}(\lambda) |\Phi\rangle\langle\Phi| \tag{3.2.4}$$

note that both sides are positive. The above equation must be satisfied for all $|\Phi\rangle$. This can only be true when $c_l |\Phi\rangle = \lambda_l |\Phi\rangle$ and $\sum_l g_l |\lambda_l|^2 = \mathrm{Re}(\lambda)$. □

We define a **dark state** as a state that is an eigenstate of a Hamiltonian ($H^{(D)}$) and set of jump operators ($c_l^{(D)}$). Rearranging conditions (1) and (2)

$$\begin{aligned} H^{(D)}|\Phi\rangle &= \mathrm{Im}\{\lambda\}|\Phi\rangle \\ c_l^{(D)}|\Phi\rangle &= 0 \end{aligned} \tag{3.2.5}$$

the steady state, $|\Phi\rangle$, is an eigenstate of the Hamiltonian $H^{(D)} = H - i\sum_l g_l \lambda_l (c_l')^\dagger + i\sum g_l \lambda_l^* c_l$, and a null ket of the jump operator $c_l^{(D)} = c_l - \lambda_l$. Physically these conditions mean, in addition to being a stationary state of the unitary dynamics, a dark state cannot absorb or emit a photon.

3.3 Adiabatic Elimination of Reservoir

We consider a general adiabatic elimination of a low/medium Q-value resonator mode, coupled to an arbitrary system $\mathcal{S}$ with a weak Jaynes-Cummings interaction. Due to the low Q-value of the resonator, we assume weak coupling i.e. $\kappa \gg g$. In this regime, the following ansatz is valid

$$\chi \approx \rho_S(t) \otimes |0\rangle_R \langle 0| . \tag{3.3.1}$$

We consider the Hamiltonian

$$H = H_S + H_R + H_{SR} \tag{3.3.2}$$

where

$$\begin{aligned} \frac{H_R}{\hbar} &= \Delta b^\dagger b \\ \frac{H_{SR}}{\hbar} &= g\left(b^\dagger \hat{S} e^{i\phi} + b\hat{S}^\dagger e^{-i\phi}\right). \end{aligned} \tag{3.3.3}$$

and $\hat{S}$ is an arbitrary system operator ($\hat{S} \in \mathcal{H}_S$). The quantum master (GKSL) equation, expressed in superoperator notation, with resonator decay is

$$\begin{aligned} \frac{d}{dt}\chi &= (\mathcal{L}_R + \mathcal{L}_S + \mathcal{L}_{SR})\,\chi \\ \mathcal{L}_R\bullet &= -\frac{i}{\hbar}[H_R, \bullet] + \kappa\mathcal{D}[b]\,\bullet \\ \mathcal{L}_S\bullet &= -\frac{i}{\hbar}[H_S, \bullet] \\ \mathcal{L}_{SR}\bullet &= -\frac{i}{\hbar}[H_{SR}, \bullet]. \end{aligned} \tag{3.3.4}$$

Moving into the interaction picture, we can write

$$\begin{aligned} \tilde{\chi} &= e^{-(\mathcal{L}_S+\mathcal{L}_R)t}\chi \\ \frac{d}{dt}\tilde{\chi} &= \tilde{\mathcal{L}}_{SR}(t)\tilde{\chi} \\ \tilde{\mathcal{L}}_{SR}(t) &= e^{-(\mathcal{L}_S+\mathcal{L}_R)t}\mathcal{L}_{SR}e^{(\mathcal{L}_S+\mathcal{L}_R)t}. \end{aligned} \tag{3.3.5}$$

Using the factorization property of superoperators, namely $AB\bullet = (A\bullet)(B\bullet)$ and $\bullet AB = (\bullet A)(\bullet B)$, $\tilde{\mathcal{L}}_{RS}(t)$ can be factorized into time-dependent system and reservoir superoperators.

$$\begin{aligned} \tilde{\mathcal{L}}_{SR}(t) &= -ig\{\mathcal{R}_2'(t)\mathcal{S}_1'(t)e^{i\phi} + \mathcal{R}_1'(t)\mathcal{S}_2'(t)e^{-i\phi} - \mathcal{R}_2'^\dagger(t)\mathcal{S}_1'^\dagger(t)e^{-i\phi} - \mathcal{R}_1'^\dagger(t)\mathcal{S}_2^\dagger(t)e^{i\phi}\} \\ &= -ig\left[(b^\dagger\bullet)'(\hat{S}\bullet)'e^{i\phi} - (\bullet b^\dagger)'(\bullet\hat{S})'e^{i\phi} + (b\bullet)'(\hat{S}^\dagger\bullet)'e^{-i\phi} - (\bullet b)'(\bullet\hat{S}^\dagger)'e^{-i\phi}\right] \\ \mathcal{S}_1'(t) &= (\hat{S}\bullet)' = e^{-\mathcal{L}_S t}\hat{S}\bullet e^{\mathcal{L}_S t} \\ \mathcal{R}_1'(t) &= (b\bullet)' = e^{-\mathcal{L}_R t}b\bullet e^{\mathcal{L}_R t} \\ \mathcal{S}_2'(t) &= (\hat{S}^\dagger\bullet)' = e^{-\mathcal{L}_S t}\hat{S}^\dagger\bullet e^{\mathcal{L}_S t} \\ \mathcal{R}_2'(t) &= (b^\dagger\bullet)' = e^{-\mathcal{L}_R t}b^\dagger\bullet e^{\mathcal{L}_R t} \end{aligned}$$

Time dependent superoperators of the form $\mathcal{O}(t) = e^{-\mathcal{L}t} S e^{\mathcal{L}t}$ satisfy Heisenberg-like equation

$$\frac{d}{dt}\mathcal{O}(t) = [\mathcal{O}, \mathcal{L}]. \tag{3.3.6}$$

Sparing the reader, we relegate the mathematical details to Appendix B, and directly present the final solutions to the operators below:

$$\begin{aligned}
\mathcal{R}_1'(t) &= (b\bullet)' = (b\bullet)\, e^{-\left(i\Delta+\frac{\kappa}{2}\right)t} \\
\mathcal{R}_1'^{\dagger}(t) &= \left(\bullet b^\dagger\right)' = \left(\bullet b^\dagger\right) e^{\left(i\Delta-\frac{\kappa}{2}\right)t} \\
\mathcal{R}_2'(t) &= \left(b^\dagger\bullet\right)' = \left(b^\dagger\bullet\right) e^{(i\Delta+\frac{\kappa}{2})t} - \left(\bullet b^\dagger\right) e^{i\Delta t}\left(e^{\kappa t/2} - e^{-\kappa t/2}\right) \\
\mathcal{R}_2'^{\dagger}(t) &= (\bullet b)' = (\bullet b)\, e^{\left(-i\Delta+\frac{\kappa}{2}\right)t} - (b\bullet)\left(e^{\kappa t/2} - e^{-\kappa t/2}\right).
\end{aligned} \tag{3.3.7}$$

As a check, note that $(b\bullet)' = (b\bullet)$ and $\left(b^\dagger\bullet\right)' = (b^\dagger\bullet)$ at $t = 0$.

Substituting the above solutions in Eq. (3.3.5) and tracing over the reservoir to capture the effective dynamics of the reduced system, we obtain

$$\frac{d}{dt}\tilde{\rho}_S = \int_0^t d\tau\; tr_R\left\{\tilde{\mathcal{L}}_{SR}(t)\tilde{\mathcal{L}}_{SR}(\tau)\tilde{\rho}_S(t)\left|0\right\rangle_R\left\langle 0\right|\right\}. \tag{3.3.8}$$

Note that $tr_R\left\{\tilde{\mathcal{L}}_{SR}(t)\tilde{\rho}_S(t)\left|0\right\rangle_R\left\langle 0\right|\right\} = 0$ because $\langle 0|b|0\rangle = \langle 0|b^\dagger|0\rangle = 0$. We find that second-order product is decaying as the time difference $t - \tau$ increases. This is the reservoir correlation function.

$$\begin{aligned}
tr_R\{\tilde{\mathcal{L}}_{SR}(t)\tilde{\mathcal{L}}_{SR}(\tau)\tilde{\chi}\} = g^2 e^{-\kappa(t-\tau)/2}\{&\mathcal{S}_1'^{\dagger}(t)\mathcal{S}_1'(\tau) \\
&+ \mathcal{S}_1'(t)\mathcal{S}_1'^{\dagger}(\tau) - \mathcal{S}_2'^{\dagger}(t)\mathcal{S}_1'^{\dagger}(\tau) - \mathcal{S}_2'(t)\mathcal{S}_1'(t)\}\tilde{\rho}_S(t)
\end{aligned} \tag{3.3.9}$$

In the Markovian limit, the correlation function decays instantaneously i.e. $e^{-\kappa(t-\tau)/2} \to 2\delta(t-\tau)/\kappa$. This leads us to the following equation [8, 13] for the system density operator,

$$\frac{d}{dt}\tilde{\rho}_S = \frac{2g^2}{\kappa}\{2\mathcal{S}_1'^{\dagger}(t)\mathcal{S}_1(t) - \mathcal{S}_2'^{\dagger}(t)\mathcal{S}_1'^{\dagger}(t) - \mathcal{S}_2'(t)\mathcal{S}_1'(t)\}\tilde{\rho}_S(t) \tag{3.3.10}$$

Substituting the definitions of $\mathcal{S}_1'(t)$ and $\mathcal{S}_2'(t)$, remembering $\rho_S = e^{\mathcal{L}_S t}\tilde{\rho}_S$, taking a derivative, simplifying, rearranging, and using $\mathcal{L}_S\rho_S = -\frac{i}{\hbar}[H_S, \rho_S]$ we arrive at

$$\begin{aligned}\frac{d}{dt}\rho_S &= -\frac{i}{\hbar}[H_S, \rho_S] + \frac{2g^2}{\kappa}\left\{2\hat{S}\rho_S\hat{S}^\dagger - \hat{S}^\dagger\hat{S}\rho_S - \rho_S\hat{S}^\dagger\hat{S}\right\} \\ &= -\frac{i}{\hbar}[H_S, \rho_S] + \frac{4g^2}{\kappa}\mathcal{D}[\hat{S}]\rho_S. \end{aligned} \tag{3.3.11}$$

The reduced system undergoes unitary evolution in conjunction with dissipative process given by the "engineered" jump operator $\hat{S}$. Furthermore, adiabatic elimination allows us to read off the "engineered" dissipation rate seen by the system as $\Gamma = \frac{4g^2}{\kappa}$. Our next task is to find the operator $\hat{S}$ that makes a two-qubit system decay into a Bell state.

3.4 Bell State Stabilization

3.4.1 Symmetric Scheme

We will consider two driven qubits interacting with a single resonator mode, as depicted in Fig. 3.1(a). This is a standard situation encountered in platforms such as circuit-QED [14]. The lab frame Hamiltonian describing the system is,

$$\frac{H}{\hbar} = \omega_c b^\dagger b + \sum_{i=1}^{2}\left\{\frac{\omega_i}{2}\sigma_{zi} + \Omega_i\cos\left(\omega_{li}t\right)\sigma_{xi} + g_i\sigma_{xi}\left(b + b^\dagger\right)\right\}. \tag{3.4.1}$$

We avoid the fast dynamics caused by the drives by changing into a rotating frame with the unitary

$$U = \exp\left(-i\left\{\omega_c b^\dagger b + \sum_{i=1}^{2}\frac{\omega_{li}}{2}\sigma_{zi}\right\}\right). \tag{3.4.2}$$

Transforming the Hamiltonian in this frame as $H' = \mathcal{U}H\mathcal{U}^\dagger - H_{rot}$ (see Appendix A) and performing RWA, we find

$$\begin{aligned} \frac{H'_R}{\hbar} &= 0 \\ \frac{H'_S}{\hbar} &\approx \sum_{i=1}^{2}\left(\frac{\delta_i}{2}\sigma_{zi} + \frac{\Omega_i}{2}\sigma_{xi}\right) \\ \frac{H'_{SR}}{\hbar} &\approx b^\dagger \underbrace{(g_1\sigma_1 + g_2\sigma_2)}_{=g\hat{S}} + h.c. \end{aligned} \tag{3.4.3}$$

with detunings $\delta_i = \omega_i - \omega_{li}$. Note that we have assumed resonance between the cavity and qubit driving field, i.e., $\omega_c = \omega_{l1} = \omega_{l2}$. Comparing the interaction Hamiltonian with Eq. (3.3.3) we conclude that the effective jump operator is $g\hat{S} = g_1\sigma_1 + g_2\sigma_2$ giving the engineered dissipator,

$$\mathcal{D}[\hat{S}] = \mathcal{D}[g_1\sigma_1 + g_2\sigma_2]. \tag{3.4.4}$$

Writing the resultant master equation describing the two-qubit open system, we obtain

$$\begin{aligned} \dot{\rho}_S = &-\frac{i}{\hbar}[H'_S, \rho_S] + \frac{4g_1^2}{\kappa}\mathcal{D}[\sigma_1]\rho_S + \frac{4g_2^2}{\kappa}\mathcal{D}[\sigma_2]\rho_S \\ &+ \frac{4g_1g_2}{\kappa}\left[\left(\sigma_1\rho_S\sigma_2^\dagger - \frac{1}{2}\left\{\sigma_2^\dagger\sigma_1, \rho_S\right\}\right) + \left(\sigma_2\rho_S\sigma_1^\dagger - \frac{1}{2}\left\{\sigma_1^\dagger\sigma_2, \rho_S\right\}\right)\right]. \end{aligned} \tag{3.4.5}$$

where we have factored the engineered dissiparor into single-qubit and two-qubit dissipation terms explicitly. Expressed in this form each qubit experiences relaxation at rate proportional to $4g_i^2/\kappa$. The final terms in Eq. (3.4.5) give rise to a dissipative interaction (between the qubits Alice and Bob) with a strength proportional to $4g_1g_2/\kappa$ [Fig. 3.1(b)].

For the purposes of bell-state stabilization the couplings and drives need to be homogeneous. That is $g_1 = g_2 = g$, and $\Omega_1 = \Omega_2 = \Omega$. Under these conditions the jump operator $\hat{S}$ has zero eigenvalues exclusively, $\lambda_l = 0$ in Eq. (3.2.5), and its null space spans contains dark states of the form

$$|\Phi\rangle = \frac{1}{\sqrt{1+|\alpha|^2}}\left(|gg\rangle + \alpha|S\rangle\right) \tag{3.4.6}$$

where α is called the singlet fraction. Furthermore, condition *(2)* of **Theorem 1** becomes $H'_S|\Phi\rangle = 0$. This constraint on the parameters requires

$$\delta = \delta_1 = -\delta_2; \quad \text{and} \quad \alpha = \frac{\Omega}{\sqrt{2}\delta}. \tag{3.4.7}$$

When the qubit drives are strong and resonant, $|\Phi\rangle \xrightarrow{\alpha\to\infty} |S\rangle$, a high-fidelity singlet state is stabilized. This was verified numerically in Fig. 3.1(d).

3.4.2 Chiral Scheme

We again consider the system of two qubits coupled to common resonator, but with an additional time-dependent coupling between the qubits, Fig. 3.2(a). The Hamiltonian for this system is

$$\frac{H}{\hbar} = \omega_c b^\dagger b + \sum_{i=1}^{2}\left\{\frac{\omega_i}{2}\sigma_{zi} + \Omega_i \cos(\omega_{li}t)\,\sigma_{xi} + g_i\sigma_{xi}(b+b^\dagger)\right\} + M_{12}(t)\sigma_{x1}\sigma_{x2} \tag{3.4.8}$$

where $M_{12}(t) = Je^{i\omega_p t} + c.c.$ As before, we isolate the slow dynamics of the interaction by moving into a rotating frame with the unitary given in Eq. (3.4.2). Picking the modulation frequency to be the difference, $\omega_p = \omega_{l1} - \omega_{l2}$. Post RWA, the Hamiltonian is

$$\begin{aligned}
\frac{H'_R}{\hbar} &= 0 \\
\frac{H'_S}{\hbar} &= \sum_{i=1}^{2}\left(\frac{\delta_i}{2}\sigma_{zi} + \frac{\Omega_i}{2}\sigma_{x1}\right) + J\sigma_1\sigma_2^\dagger + J^*\sigma_1^\dagger\sigma_2 \\
\frac{H'_{SR}}{\hbar} &= b^\dagger(g_1\sigma_1 + g_2\sigma_2) + h.c.
\end{aligned} \tag{3.4.9}$$

The master equation for the reduced system is same as Eq. (3.4.5), since the qubit-resonator coupling remains unchanged, except with an additional coupling term in H'_S. Using it, we calculate expectation values of single qubit operators and find

$$\begin{aligned}
\frac{d}{dt}\langle\sigma_1\rangle &= -i\Delta_1\langle\sigma_1\rangle + i\Omega_1\langle\sigma_{z1}\rangle + \left(iJ^* + \frac{\Gamma}{2}\right)\langle\sigma_{z1}\sigma_2\rangle - \frac{\Gamma}{2}\langle\sigma_1\rangle \\
\frac{d}{dt}\langle\sigma_2\rangle &= -i\Delta_2\langle\sigma_2\rangle + i\Omega_2\langle\sigma_{z2}\rangle + \left(iJ + \frac{\Gamma}{2}\right)\langle\sigma_1\sigma_{z2}\rangle - \frac{\Gamma}{2}\langle\sigma_2\rangle
\end{aligned}$$

If the strength and phase of the qubit-qubit couplings are tuned such that

$$\boxed{J = \pm i\frac{\Gamma}{2}} \tag{3.4.10}$$

then one qubit sees the other but not vice versa. The boxed equation is called the chirality condition, which has previously been employed to implement nonreciprocal amplification and frequency conversion [15–17]. Assuming homogeneous drives and couplings, the dark state is the same as the symmetric case, Eq. (3.4.6). The constraint $H_S'|\Phi\rangle = 0$ implies $\delta_1 = -\delta_2 = \delta$ and [18, 19]

$$\alpha = \frac{\sqrt{2}\Omega}{2\delta + i\Gamma}. \tag{3.4.11}$$

Results of numerical simulations in Fig. 3.2(d) show that the chiral scheme stabilizes a high-fidelity singlet-state when $\alpha \to \infty$.

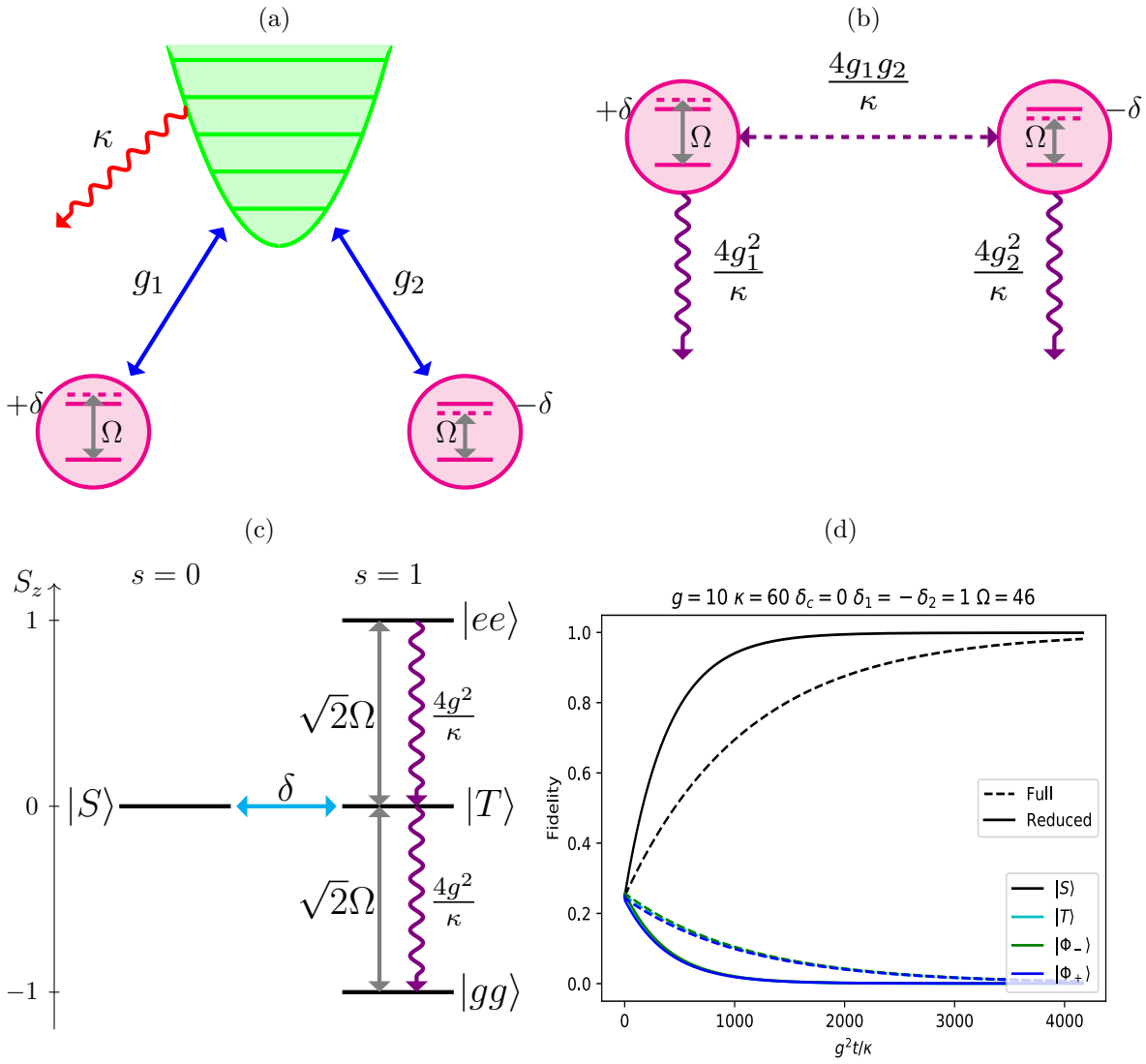

Figure 3.1: (a) Graphical depiction of two qubits coupled to a lossy resonator mode. (b) After the resonator mode is adiabatically eliminated the resonator decay (red) and the resonator-qubit interactions (blue) merge to create an engineered dissipator (purple). This "engineered" dissipator gives rise to local qubit relaxation and a dissipative interaction between qubits. (c) Graphical depiction of how the states couple for homogeneous drives and couplings. (d) Master equation simulations of both the full and reduced systems, show high-fidelity stabilization of a singlet state for strong resonant drives.

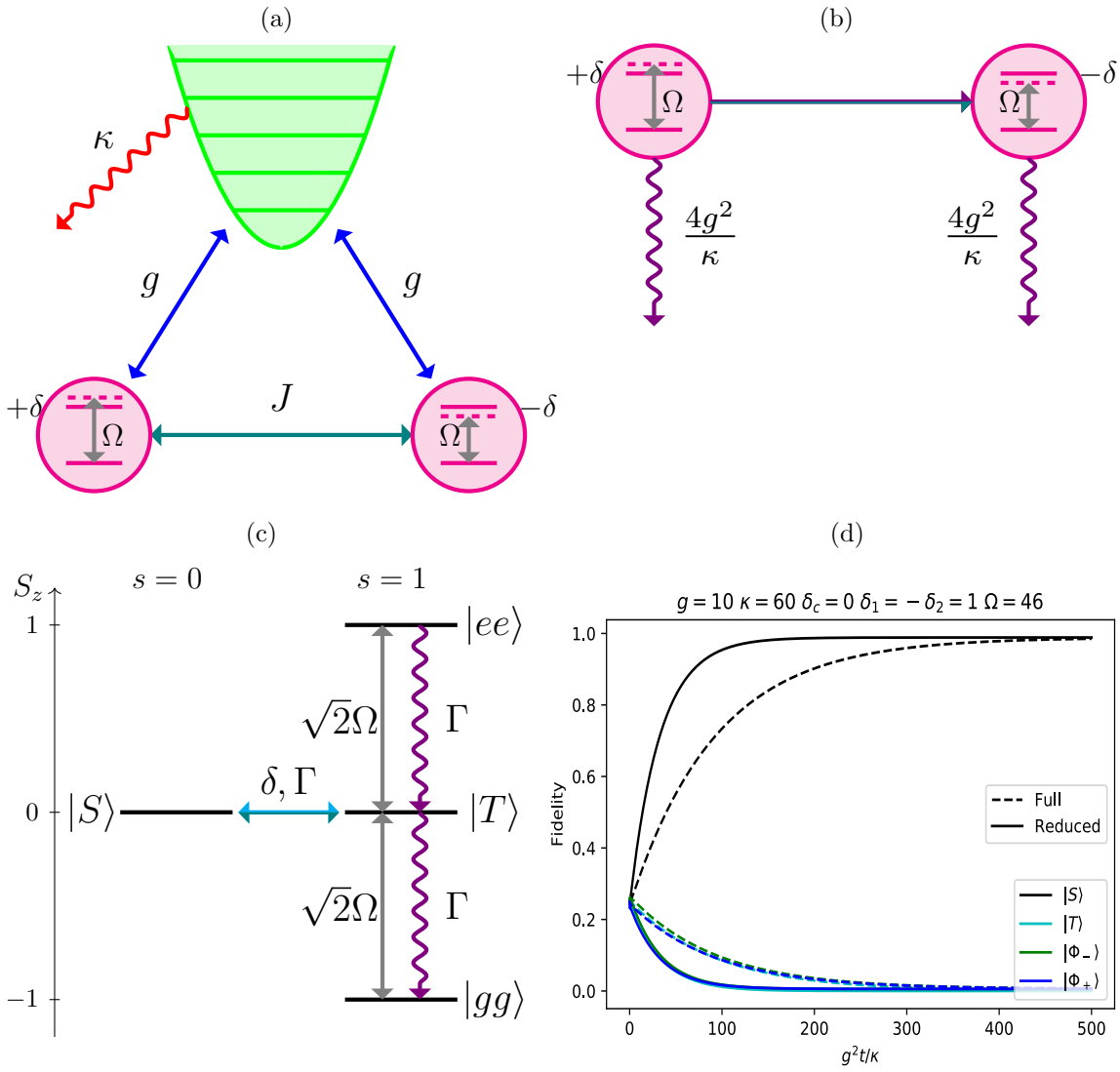

Figure 3.2: (a) Couplings for implementing chiral interaction between two qubits. The main change from Fig. 3.1 is addition of the qubit-qubit coupling J (teal arrow). (b) The parametric and dissipative interaction interfere so that the net coupling becomes unidirectional. (c) The qubit-qubit interaction adds a second coupling between states $|S\rangle \leftrightarrow |T\rangle$ proportional to Γ. (d) Master equation simulations of both the full and reduced systems, show high-fidelity stabilization of a singlet state for strong resonant drives.

3.4.3 Comparison: Symmetric vs. Chiral

Comparing the stabilization graphs of Fig. 3.1(d) and Fig. 3.2(d), we see that the chiral case stabilizes a singlet state significantly faster than its symmetric counterpart by a factor of ~ 8. The addition of the chiral coupling does cause a decrease in the steady state fidelity, but is more than made up for by the increase in speed. We can capture this idea by defining a performance metric M,

$$M = F_{|S\rangle}\frac{\Delta_{\mathcal{L}}}{\Gamma} \tag{3.4.12}$$

that quantifies the product of the fidelity and gap. We first perform an analytical calculation of this quantity for the symmetric case. The fidelity of stabilizing a singlet case can be calculated from the singlet fraction $\alpha =$ introduced earlier as [Eq. (3.4.6)],

$$F_{|S\rangle} = \frac{|\alpha|^2}{1+|\alpha|^2} = \frac{\Omega^2}{\Omega^2+2\delta^2}. \tag{3.4.13}$$

We can determine the stabilization time by taking the matrix element of Eq. (3.1.4) in the singlet state, where $P_{|S\rangle} = \langle S|\rho|S\rangle$.

$$\dot{P}_{|S\rangle} = \langle S|\mathcal{L}\rho_S|S\rangle. \tag{3.4.14}$$

We adiabatically eliminate the coherences (off-diagonal elements) and solve in terms of the populations so that the rate of preparation of the target state, $|S\rangle$, can be written as [20, 21]

$$\dot{P}_{|S\rangle} = \Gamma_{|g\rangle}P_{|gg\rangle} + \Gamma_{|S\rangle}P_{|S\rangle} + \Gamma_{|T\rangle}P_{|T\rangle} + \Gamma_{|ee\rangle}P_{|ee\rangle}. \tag{3.4.15}$$

Since the ground (or excited) state is farthest from the target state, one can obtain an upper bound for the stabilization rate by considering the rate of preparation of singlet if the system is initialized in $\rho_S(0) = |gg\rangle\langle gg|$, i.e. $\Gamma_{|gg\rangle} \geq \Delta_{\mathcal{L}}$ [21]. For the symmetric case,

$$\Delta_{\mathcal{L}} \leq \Gamma_{|gg\rangle} \approx \frac{\Gamma^3}{\Gamma^2+2\Omega^2}. \tag{3.4.16}$$

where we have performed a series expansions in the small parameter δ/Ω and retained only the zeroth order term. Fig. 3.3(a) shows a plot of the metric M calculated using

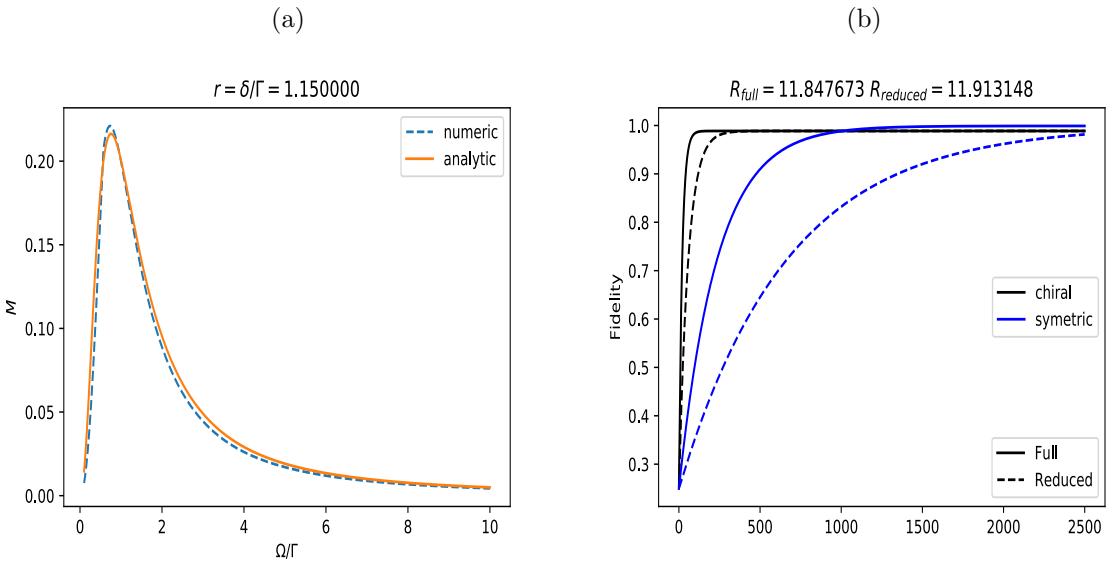

Figure 3.3: (a) Performance metric $M = F_{|S\rangle}\Delta_{\mathcal{L}}/\Gamma$ for the symmetric case, plotted as a function of Ω/Γ. The agreement between analytical and numerical results is good, though deviations can be seen away from optimal Ω/Γ. (b) Performance metric M for chiral scheme is better by a factor of $R = \frac{M_{chiral}}{M_{sym}} \sim 12$, as seen from calculations performed for both the full and reduced system. The parameters used for simulations are the same as that used to generate Figs. 3.1(d) and 3.2(d).

Eqs. (3.4.13) and (3.4.16) for the symmetric scheme, and compares it with the values obtained from a master equation simulation of the reduced system.

Fig. 3.3(b) shows a comparison of the symmetric and chiral schemes for the same system parameters. As is evident, chiral scheme performs quantitatively better as captured by the ratio of the performance metrics

$$R = \frac{M_{\text{chiral}}}{M_{\text{sym}}} \approx 12. \tag{3.4.17}$$

Chapter 4

Multipartite Entanglement Stabilization

The central goal of quantum optics is to develop "tools" to control light-matter interactions at the single quanta level. Chiral interfaces, such as light scattering off an atom and the photoelectric effect, are interesting examples where photon emission and absorption is non-reciprocity arising from the polarization-dependent coupling strength. These phenomena are dealt within the framework of *chiral quantum optics*. For our purposes we'll be interested 'one-dimensional' interfaces where quantum emitters (atoms/qubits) interact with guided modes of light with in a waveguide. These system display unidirectional emission and absorption where an emitter can interact with another emitter, via a photon, only if it is further down the chain. Theses systems naturally give rise to chiral couplings [18, 22].

Building upon ideas developed in the last chapter, we will consider a chain of a qubits coupled to mutual resonator that realizes pairwise chiral couplings between qubits to create effective unidirectional emission and absorption within the qubit system. We find that in the chiral system, the nature of entanglement can be modified from two-qubit to multi-qubit by selecting the suitable driving condition: specifically, the detunings of the driving fields from respective qubit frequencies. The nature of

the entanglement generated in steady state will be investigated by looking at purity of qubit subspaces spanning 1, 2, 3 and 4 qubits respectively. We will also comment on how multipartite entanglement can be realized without chirality, though at the cost of introducing additional constraints on the system.

4.1 Four-qubit engineered dissipator

Consider a chain of four qubits interacting with a mutual resonator, as depicted in system Fig. 4.1(a). We assume homogeneous couplings, $g_i = g$, so

$$\frac{H'_{SR}}{\hbar} = gb^\dagger(\sigma_1 + \sigma_2 + \sigma_3 + \sigma_4) + h.c. \tag{4.1.1}$$

Using the adiabatic elimination of the resonator, as described in the previous chapter, this allows a straightforward identification of the effective junp operator

$$\hat{S} = g(\sigma_1 + \sigma_2 + \sigma_3 + \sigma_4) \tag{4.1.2}$$

which leads to the following master equation for the reduced system

$$\dot{\rho}_S = -\frac{i}{\hbar}[H'_S, \rho_S] + \Gamma\mathcal{L}[\sigma_1 + \sigma_2 + \sigma_3 + \sigma_4]\rho_S. \tag{4.1.3}$$

As before, $\Gamma = \frac{4g^2}{\kappa}$ is the engineered dissipation rate. Associated with each of the qubits is a detuning, δ_α, also depicted in in Fig. 4.1(a). These detunings must come in equal and opposite pairs to form a perfectly coherent emitter-absorber with no spontaneous emission into the guided mode [23]. That is for each qubit j with a detuning δ_j, there is another qubit l in the chain with $\delta_j = -\delta_l$.

We will again consider the stabilization dynamics for both:

- a symmetric interaction between each pair of qubits, for which the qubit Hamiltonian is invariant under pairwise permutations [Fig. 4.1(b)],

$$H_{sym} = \sum_i \left(\frac{\delta_i}{2}\sigma_{zi} + \frac{\Omega}{2}\sigma_{xi}\right) \tag{4.1.4}$$

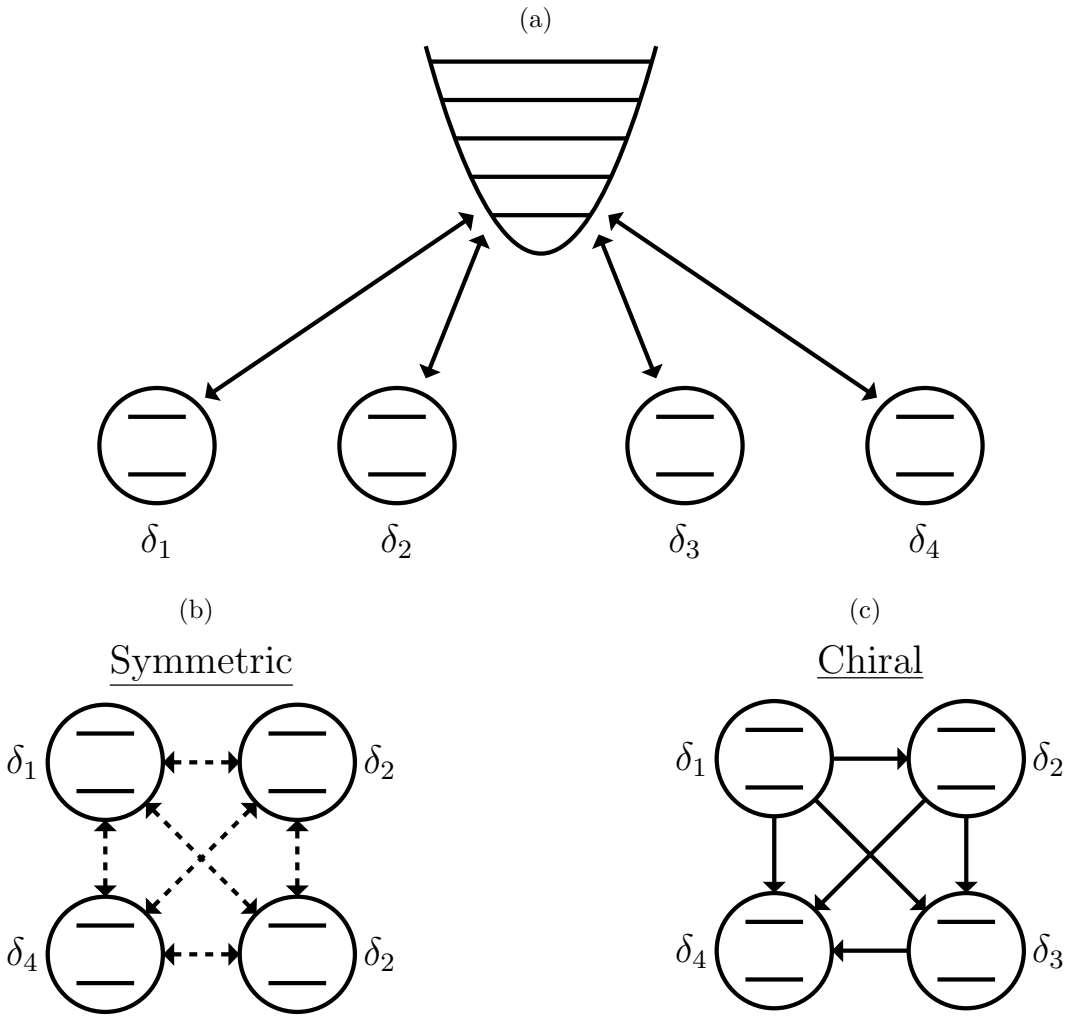

Figure 4.1: Four qubits coupled to a mutually shared resonator mode, with an associated detuning pattern $(\delta_1, \delta_2, \delta_3, \delta_4)$. (b) In the symmetric scheme all qubits are coupled to each other through a dissipative coupling. (c) Addition of qubit-qubit couplings, and their interference with the dissipative couplings, renders all pairwise couplings in the chain unidirectional, such that the qubits on the left cannot "see" the qubits to their right.

- a chiral interaction between each pair of qubits, for which the qubit Hamiltonian is no longer invariant under pairwise permutations [Fig. 4.1(c)],

$$H_{chiral} = H_{sym} - i\frac{\Gamma}{2}\sum_{i>j}\left(\sigma_j^\dagger\sigma_i - \sigma_j\sigma_i^\dagger\right) \tag{4.1.5}$$

This is because the qubit-qubit couplings pick up a phase under an index swap. Recall that the combination of these couplings with engineered dissipation creates unidirectional emission and absorption from left-to-right in the chain, as demonstrated for the Bell state stabilization in the last chapter.

4.2 Role of chirality

We consider the entanglement dynamics in the symmetric and chiral case for two different types of detuning patterns: alternating and staggered. An alternating detuning pattern is of the form $(\delta_a, -\delta_a, \delta_b, -\delta_b)$. A staggered detuning is obtained by permuting two of the detunings: $(\delta_a, \delta_b, -\delta_a, -\delta_b)$.

4.2.1 Entanglement Identification

In order to identify the nature of multipartite entanglement in each case, we use a quantity called the purity of the density matrix: $tr\,(\rho^2)$. The purity of the density matrix has the following property

$$\begin{aligned} tr(\rho^2) &= 1 \quad \text{for a pure state} \\ tr(\rho^2) &< 1 \quad \text{for a mixed state.} \end{aligned}$$

Now suppose two subsystem in the chain are entangled. Then by definition the total state, $|\Phi\rangle$, cannot written as a product state of the two subsystems. That is

$$|\Phi\rangle \neq |\phi_1\rangle \otimes |\phi_2\rangle. \tag{4.2.1}$$

Therefore when one of the subsystems is traced over, the resulting density matrix is mixed with a purity less than one [24]. For example, suppose two qubits j and k in

the chain are entangled.

$$|S\rangle_{jk} = \frac{1}{\sqrt{2}} \left(|ge\rangle_{jk} - |eg\rangle_{jk} \right) \tag{4.2.2}$$

We trace over the subspace j and find

$$\rho_k = tr_j\{|S\rangle_{jk}\langle S|\} = \frac{1}{2} \left(|e\rangle_k\langle e| + |g\rangle_k\langle g| \right) = \frac{1}{2} \begin{pmatrix} 1 & 0 \\ 0 & 1 \end{pmatrix}. \tag{4.2.3}$$

Computing $tr_k \{\rho_k^2\} = 0.5 < 1$, we see that the subsystem is mixed and its purity is less than one.

4.2.2 Alternating Detunings

The results for purity plots are shown in Fig. 4.2. Our results show that both the symmetric and chiral schemes purify the state $|S\rangle_{12}|S\rangle_{34}$. However, the chiral purification is faster by more than a factor of 10. Furthermore, in the chiral case $|S\rangle_{12}$ is stabilized before $|S\rangle_{34}$ displaying the system's unidirectional nature.

4.2.3 Staggered Detunings

The results for purity plots are shown in Fig. 4.3. For the symmetric coupling case we get non-local (though still pairwise) entanglement, and the state $|S\rangle_{13}|S\rangle_{24}$ is purified. However, for chiral couplings, only the full 4-qubit system purity goes to one indicating that the steady state exhibits genuine four-qubit entanglement.

4.3 Caveat: Symmetric Four-qubit Entanglement

Consider the homogeneous detuning detuning pattern

$$(\delta, \delta, -\delta, -\delta). \tag{4.3.1}$$

The third and fourth qubit can both form a coherent emitter-absorber pair with the first qubit because the detunings are equal and opposite. In other words, the first

(a)

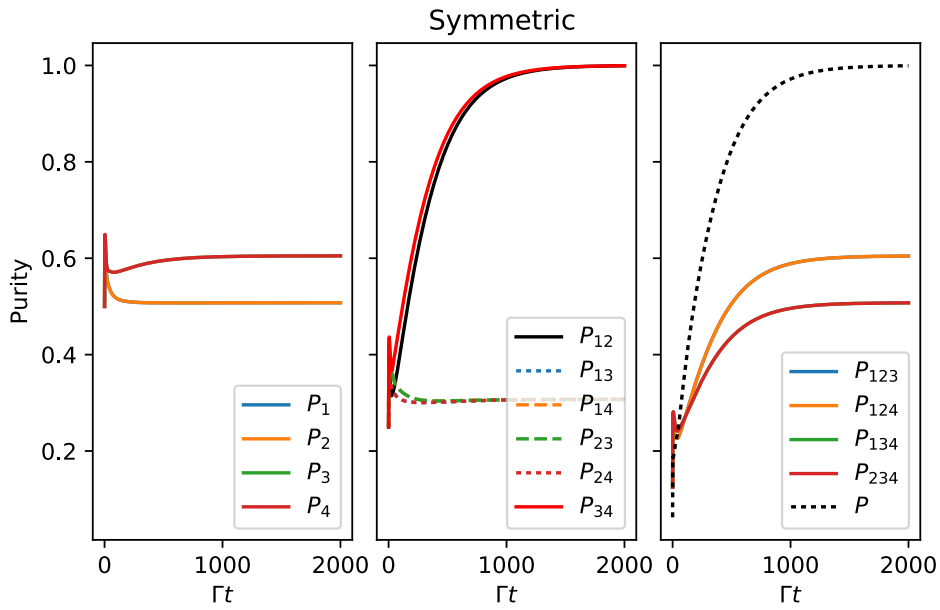

(b)

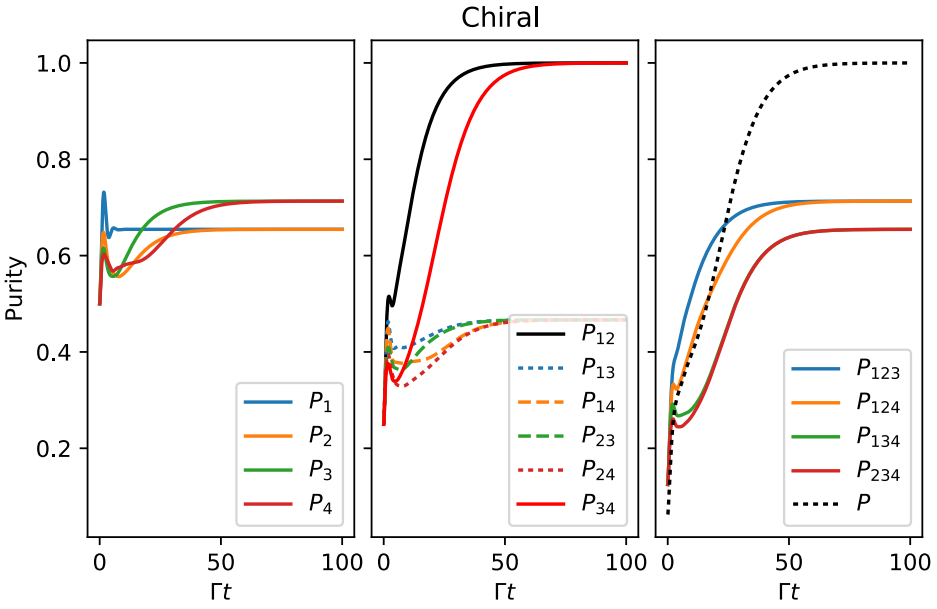

Figure 4.2: Time-domain simulations of a four-qubit chain for symmetric and chiral cases with alternating detuning pattern: $(\delta_a, -\delta_a, \delta_b, -\delta_b)$. All the plots were generated with the same parameters, $\Gamma = 4\frac{g^2}{\kappa} = 10,\ \delta_a = 1,\ \delta_b = 4,\ \Omega = 8$.

qubit can become entangled with the third qubit or the forth qubit. Because there can be no preferred entangled state, we found that the steady state was a superposition

(a)

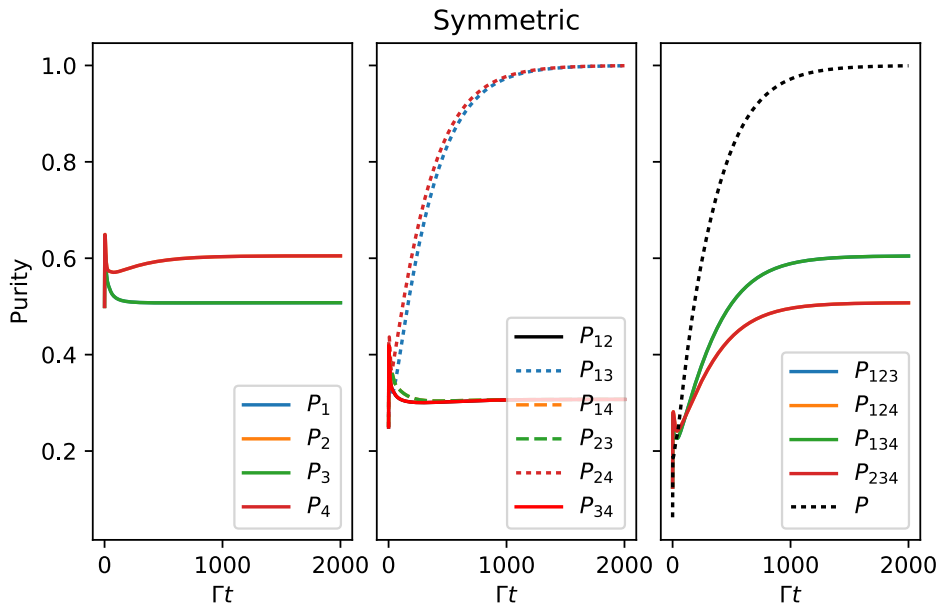

(b)

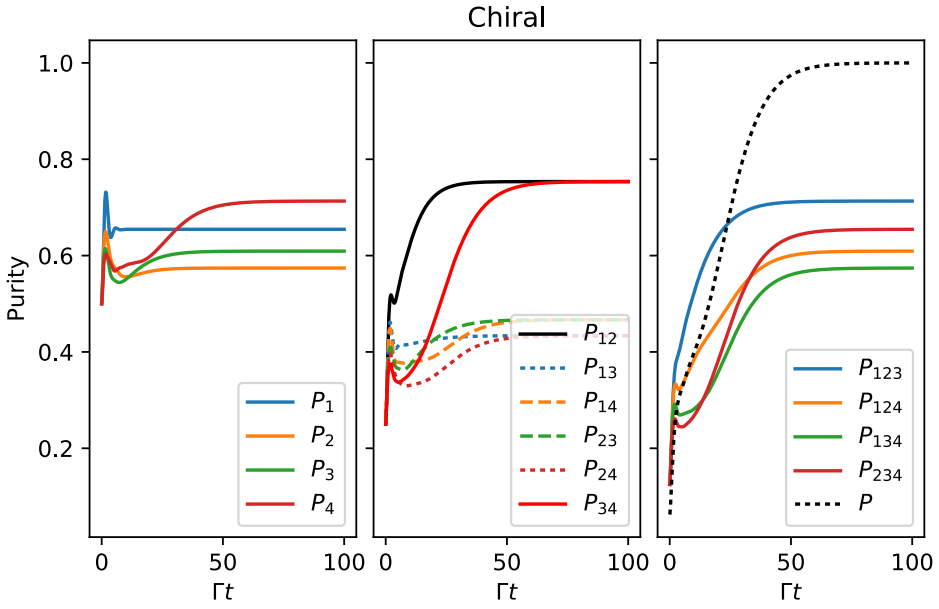

Figure 4.3: Time-domain simulations of a four-qubit chain for symmetric and chiral cases with staggered detuning pattern, $(\delta_a, \delta_b, -\delta_a, -\delta_b)$. All the plots were generated with the same parameters, $\Gamma = 4\frac{g^2}{\kappa} = 10,\ \delta_a = 1,\ \delta_b = 4,\ \Omega = 8$.

of the two possible configurations. Thus the detuning pattern, Eq. (4.3.1), stabilizes

$$\frac{1}{\sqrt{2}}\left(|S\rangle_{13}|S\rangle_{24} + |S\rangle_{14}|S\rangle_{23}\right). \tag{4.3.2}$$

Detuning Pattern	Stabilized State
$(\delta, -\delta, \delta, -\delta)$	$\|S\rangle_{12}\|S\rangle_{34} - \|S\rangle_{14}\|S\rangle_{23}$
$(\delta, -\delta, -\delta, \delta)$	$\|S\rangle_{12}\|S\rangle_{34} + \|S\rangle_{13}\|S\rangle_{24}$
$(\delta, \delta, -\delta, -\delta)$	$\|S\rangle_{13}\|S\rangle_{24} + \|S\rangle_{14}\|S\rangle_{23}$

Table 4.1: Table of detuning patterns and corresponding stabilized four-qubit entangled state).

However, for this scheme to work the system has to be initialized in the ground state, i.e.

$$\rho_S(0) = |gggg\rangle\langle gggg|. \tag{4.3.3}$$

We found a significant decrease in steady state fidelity when intialized in a mixed state. Table 4.1 summarizes the different permutations of the detuning pattern and the corresponding four-qubit entangled states that get stabilized as a result.

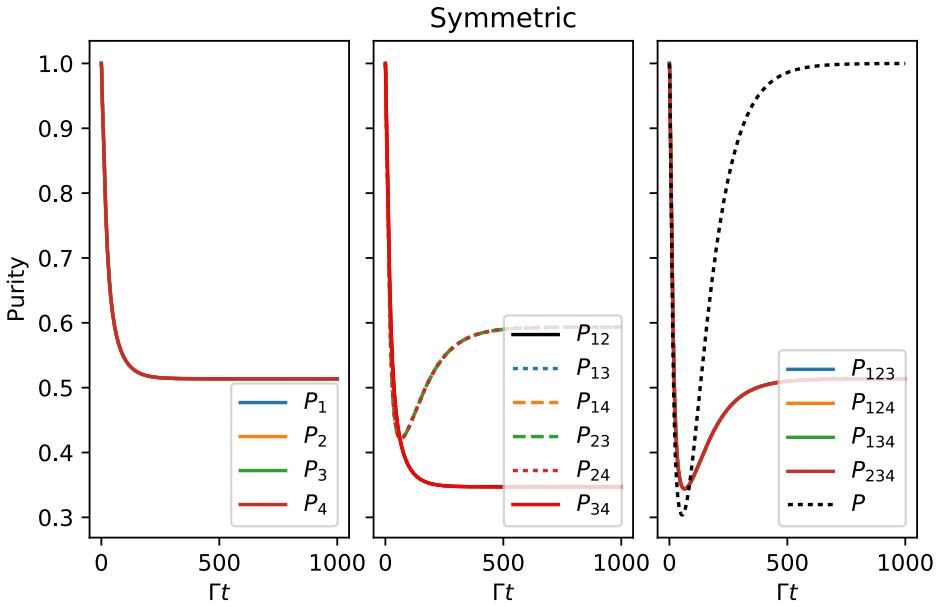

Figure 4.4: Purity plots show that the steady state is a four-qubit entangled state when the system is initialized in the ground state, and the detuning pattern is homogeneous. The parameters used for the simulation were $\Gamma = 4\frac{g^2}{\kappa} = 10,\ \delta = 1,\ \Omega = 8.$

Chapter 5

Conclusion

In conclusion, we have shown that even though dissipation can lead to decohernce that washes away quantum information, it possible to use dissipation to our advantage to stabilize entanglement with high-fidelity. Specifically, we presented schemes for two- and four-qubit entanglement generation, employing an "engineered" qubit-reservoir coupling. The reservoir in question can be implemented via a lossy harmonic oscillator. Such a scheme is compatible with standard circuit-QED platforms using microwave resonators and superconducting qubits.

We showed how the method of adiabatic elimination provides a convenient route to identify "engineered" jump operator that captures the effective dissipation seen by the qubits. This allows us to study open system dynamics of only the reduced system of interest, giving considerable advantage in terms of both analytical tractability and numerical computation. We found that for parameters considered here, entanglement stabilization with chiral qubit interactions outperforms the scheme that relies on symmetric qubit interactions. This was quantified in terms of a new performance metric M: realizing a large value of this metric entails a *simultaneous* maximization of fidelity and rate of stabilization. The chiral scheme had a performance metric that was 10x bigger than the symmetric scheme for optimal parameters.

Furthermore, four-qubit studies show that chirality is essential to purify mixtures

into genuine multipartite entangled states. The 'knob' that determines the nature of entanglement in a 1D chiral qubit chain is the detuning pattern of the driving field: if the detunings are "alternating" the qubits stabilize into pairs of singlets, while when the detunings are "staggered" (realized by permuting one of the detunings), the steady state is a true tetramer. Multipartite entanglement stabilization may be possible from symmetric dissipative interactions alone, but this requires specific driving conditions along with initial state preparation. We also find that the time scales and dynamics in qubits chains are qualitatively different with and with out chirality, which will form the basis of future investigations.

Appendix A

Rotating Frames

Let us start with the Schrodinger equation in a stationary frame

$$i\hbar\frac{d}{dt}\left|\Psi\right\rangle = H\left|\Psi\right\rangle. \tag{A.0.1}$$

we desire to transform it into a rotating frmae using a unitary operator of the form

$$\hat{U} = \exp\left(i\hat{G}t/\hbar\right), \tag{A.0.2}$$

with $\hat{G}$ clearly being self-adjoint. We now define the rotating state vector

$$\left|\tilde{\Psi}\right\rangle = \hat{U}\left|\Psi\right\rangle. \tag{A.0.3}$$

We now need to find the transformed Hamiltonian $\tilde{H}$ by constructing the Schrodinger Equation in a rotating frame. To this end, we substitute Eq. (A.0.3) in Eq. (A.0.1)

$$\begin{aligned}
i\hbar\frac{d}{dt}\left(\hat{U}^\dagger|\tilde{\Psi}\rangle\right) &= H\hat{U}^\dagger|\tilde{\Psi}\rangle \\
i\hbar\hat{U}^\dagger\frac{d}{dt}|\tilde{\Psi}\rangle + i\hbar\frac{d\hat{U}^\dagger}{dt}|\tilde{\Psi_R}\rangle &= H\hat{U}^\dagger|\tilde{\Psi}\rangle \\
\hat{U}^\dagger\left(i\hbar\frac{d}{dt}|\tilde{\Psi}\rangle\right) &= H\hat{U}^\dagger|\tilde{\Psi}\rangle - i\hbar\frac{d\hat{U}^\dagger}{dt}|\tilde{\Psi}\rangle \\
i\hbar\frac{d}{dt}|\tilde{\Psi}\rangle &= \left(\hat{U}H\hat{U}^\dagger - i\hbar\hat{U}\frac{d\hat{U}^\dagger}{dt}\right)|\tilde{\Psi}\rangle.
\end{aligned} \tag{A.0.4}$$

Comparing the Schrodinger Equation in a rotating frame

$$i\hbar\frac{d}{dt}|\tilde{\Psi}\rangle = \tilde{H}|\tilde{\Psi}\rangle \tag{A.0.5}$$

to Eq. (A.0.4) we conclude that the rotating frame Hamiltonian is

$$\tilde{H} = \hat{U}H\hat{U}^{\dagger} - i\hbar\hat{U}\frac{d\hat{U}^{\dagger}}{dt} = \hat{U}H\hat{U}^{\dagger} - \hat{G}. \tag{A.0.6}$$

Appendix B

Superoperator Algebra

Superoperators act on operators to produce new operators, just as operators act on vectors to produce new vectors. The key difference is that superoperators "embrace" their arguments. How they are embraced is conveyed using a dot notation.

$$\left(a^{\dagger 2} b \bullet\right) \hat{O} \equiv a^{\dagger 2} b \hat{O} \qquad \left(a \bullet a^{\dagger}\right) \hat{O} \equiv a \hat{O} a^{\dagger} \qquad \left(\bullet b^{\dagger} b\right) \hat{O} \equiv \hat{O} b^{\dagger} b. \tag{B.0.1}$$

Superoperator products are evaluated by substituting the superoperator, on the right, where the dot is, on the left.

$$\left(a^{\dagger 2} \bullet\right)(b \bullet) = \left(a^{\dagger 2} b \bullet\right) \qquad (a \bullet)\left(\bullet a^{\dagger}\right) = \left(a \bullet a^{\dagger}\right) \qquad (\bullet b)\left(\bullet b^{\dagger}\right) = \left(\bullet b^{\dagger} b\right) \tag{B.0.2}$$

It is also possible to work in the reverse direction and "factorize" a superoperator into products.

In general two superoperators do not commute. However, if every operators in a superoperators commutes with every operator in another superoperator then the superoperators commute. For example

$$\begin{aligned} \left(a \bullet a^{\dagger}\right)\left(b \bullet b^{\dagger}\right) &= \left(ab \bullet b^{\dagger} a^{\dagger}\right) = \left(ba \bullet a^{\dagger} b^{\dagger}\right) \\ &= \left(b \bullet b^{\dagger}\right)\left(a \bullet a^{\dagger}\right). \end{aligned} \tag{B.0.3}$$

Given a superoperators S, we associate with it a conjugate superoperator, $S^{\dagger}$. Consider

$$\left(S \hat{O}\right)^{\dagger} \equiv S^{\dagger} \hat{O}^{\dagger} = S^{\dagger} \hat{O} \tag{B.0.4}$$

where the operator $\hat{O}$ is assumed to be hermitian because $\hat{O}$ will typically be a density operator. Consider the example

$$\begin{aligned}\left(\left(a^{\dagger 2}b\bullet\right)\hat{O}\right)^{\dagger} &= \left(a^{\dagger 2}b\hat{O}\right)^{\dagger} = \left(\hat{O}^{\dagger}b^{\dagger}a^{2}\right) \\ &= \left(\bullet b^{\dagger}a^{2}\right)\hat{O} \end{aligned} \tag{B.0.5}$$

thus

$$\left(a^{\dagger 2}b\bullet\right)^{\dagger} = \left(\bullet b^{\dagger}a^{2}\right). \tag{B.0.6}$$

We can write the above equation in the form

$$\left[\left(a^{\dagger 2}\bullet\right)(b\bullet)\right]^{\dagger} = \left[\left(\bullet a^{2}\right)\left(\bullet b^{\dagger}\right)\right] \tag{B.0.7}$$

from which we conclude

$$(S_1 S_2)^{\dagger} = S_1^{\dagger} S_2^{\dagger}. \tag{B.0.8}$$

Therefore the ordering of the superoperators does not change when the hermitian conjugate is taken.

We now will move on to calculating commutators of superoperators. Consider

$$\left[\left(b\bullet b^{\dagger}\right),(b\bullet)\right] = \left(b\bullet b^{\dagger}\right)(b\bullet) - (b\bullet)\left(b\bullet b^{\dagger}\right) = 0 \tag{B.0.9}$$

and

$$\begin{aligned}\left[\left(b^{\dagger}b\bullet\right),(b\bullet)\right] &= \left(b^{\dagger}b\bullet\right)(b\bullet) - (b\bullet)\left(b^{\dagger}b\bullet\right) \\ &= \left(b^{\dagger}b^{2}\bullet\right) - \left(bb^{\dagger}b\bullet\right) \\ &= \left(b^{\dagger}b\bullet - bb^{\dagger}\bullet\right)(b\bullet) \\ &= -(b\bullet). \end{aligned}$$

A time dependent operator of the form satisfies

$$S'(t) \equiv e^{-\mathcal{L}t} S e^{\mathcal{L}t} \tag{B.0.10}$$

obey's the Heisenberg equation of motion

$$\frac{d}{dt}S'(t) = [S', \mathcal{L}]\,. \tag{B.0.11}$$

We now will solve the equation of motion. Consider $\mathcal{L} = \kappa\left(2b\bullet b^\dagger - b^\dagger b\bullet - \bullet b^\dagger b\right)$ and $S'(0) = (b\bullet)$.

$$\begin{aligned}\frac{d}{dt}(b\bullet)' &= \kappa\left[(b\bullet)', 2\left(b\bullet b^\dagger\right)' - \left(b^\dagger b\bullet\right)' - \left(\bullet b^\dagger b\right)'\right] \\ &= -\kappa\,(b\bullet)'\end{aligned} \tag{B.0.12}$$

which has a solution of the form

$$S'(t) = (b\bullet)' = e^{-\mathcal{L}t}\,(b\bullet)\,e^{\mathcal{L}t} = e^{-\kappa t}\,(b\bullet)\,. \tag{B.0.13}$$

This example is simple because the superoperator $(b\bullet)'$ does not couple to other superoperators. However, in the following example $\left(b^\dagger\bullet\right)$ couples to $\left(\bullet b^\dagger\right)$.

$$\begin{aligned}\frac{d}{dt}\left(b^\dagger\bullet\right)' &= \left[\left(b^\dagger\bullet\right)', 2\left(b\bullet b^\dagger\right)' - \left(b^\dagger b\bullet\right)' - \left(\bullet b^\dagger b\right)'\right] \\ &= \kappa\left(b^\dagger\bullet\right)' - 2\kappa\left(\bullet b^\dagger\right)' \qquad \text{(B.0.14)} \\ \frac{d}{dt}\left(\bullet b^\dagger\right) &= \kappa\left[\left(\bullet b^\dagger\right)', 2\left(b\bullet b^\dagger\right)' - \left(b^\dagger b\bullet\right)' - \left(\bullet b^\dagger b\right)'\right] = -\kappa\left(\bullet b^\dagger\right)' \qquad \text{(B.0.15)}\end{aligned}$$

The solution to equation Eq. (14) can be found by substituting $\left(\bullet b^\dagger\right)' = \left(\bullet b^\dagger\right)e^{-\kappa t}$. plugging in this solution into equation (13) the solution becomes

$$\left(b^\dagger\bullet\right)' = \left(\bullet b^\dagger\right)\left(e^{-\kappa t} - e^{\kappa t}\right) + \left(b^\dagger\bullet\right)e^{\kappa t}. \tag{B.0.16}$$

Appendix C

Parametric Interactions: Stabilizing Arbitray Bell States

Two spins coupled to a mutual cavity mode can in principle stabilize any of the following bell states

$$\begin{aligned} |S\rangle &= \frac{1}{\sqrt{2}}\left(|ge\rangle - |eg\rangle\right) \\ |T\rangle &= \frac{1}{\sqrt{2}}\left(|ge\rangle + |eg\rangle\right) \\ |\Phi_-\rangle &= \frac{1}{\sqrt{2}}\left(|ee\rangle - |gg\rangle\right) \\ |\Phi_+\rangle &= \frac{1}{\sqrt{2}}\left(|ee\rangle + |gg\rangle\right) \end{aligned}$$

for a strong resonate drive. However, these states all belong to the null space of a different jump operator. For example, $(\sigma_1 - \sigma_2)|T\rangle = 0$. Because there is a phase difference between σ_1 and σ_2 in the jump operator, there needs to be a phase difference between the couplings strength. That is $g_1 = -g_2 = g$, so $\frac{H_{SR}}{\hbar} = b^\dagger(g_1\sigma_1 + g_2\sigma_2) = gb^\dagger\left(\sigma_1 - \sigma_2\right)$.

To stabilize the states $|\Phi_-\rangle$ the operator $\sigma_2 \longrightarrow \sigma_2^\dagger$, so $(\sigma_1 + \sigma_2^\dagger)|\Phi_-\rangle = 0$. This means system-reservoir interaction Hamiltonian must have the form post RWA

$$\frac{H'_{SR}}{\hbar} \approx g_2 b^\dagger(\sigma_1 + \sigma_2^\dagger) + h.c. \tag{C.0.1}$$

Bell State	Engineered Jump Operator
$\|S\rangle$	$\sigma_1 + \sigma_2$
$\|T\rangle$	$\sigma_1 - \sigma_2$
$\|\Phi_-\rangle$	$\sigma_1 + \sigma_2^\dagger$
$\|\Phi_+\rangle$	$\sigma_1 - \sigma_2^\dagger$

Table C.1: Table of bell states with corresponding jump operator. One can easily verify that the bell state is part null space the corresponding jump operator.

The system-resvoir coupling for the second qubit has now becomes an amplification Hamiltonian.

$$H_{SR}^{(2)} \approx g_2 b^\dagger \sigma_2^\dagger + h.c. \tag{C.0.2}$$

To get an amplification Hamiltonian from the lab frame Hamiltonian, Eq. (3.4.1), the static coupling g_2 must become a "parametric" time-dependent coupling. That is

$$g_2 \to g_2(t) = g_2 e^{i\omega_{p2}t} + c.c. \tag{C.0.3}$$

When we move into the rotating frame, as defined in Eq. (3.4.2), we pick the modulation frequencies to be the sum $\omega_{p2} = \omega_2 + \omega_c$. After RWA the resulting Hamiltonian is Eq. (C.0.1). To stabilize $|\Phi_+\rangle$ we make sure $g_1 = -g_2 = g$ so the effective jump operator satisfies $(\sigma_1 - \sigma_2^\dagger)|\Phi_+\rangle = 0$.

Bibliography

[1] J. Dalibard, Y. Castin, and K. Mølmer. Wave-function approach to dissipative processes in quantum optics. *Phys. Rev. Lett.*, 68:580, February 1992.

[2] R. J. Schoelkopf and S. M. Girvin. Wiring up quantum systems. *Nature Horizons*, 551:664–669, February 2008.

[3] Frank Verstraete, Michael M. Wolf, and J. Ignacio Cirac. Quantum computation and quantum-state engineering driven by dissipation. *Nature Physics*, 5:633, 2009.

[4] S. Diehl, A. Micheli, A. Kantian, B. Kraus, H. P. Büchler, and P. Zoller. Quantum states and phases in driven open quantum systems with cold atoms. *Nature Physics*, 4:878, 2008.

[5] G. Vacanti and A. Beige. Cooling atoms into entangled states. *New J. Phys.*, 11:083008, August 2009.

[6] M. J. Kastoryano, F. Reiter, and A. S. Sørensen. Dissipative preparation of entanglement in optical cavities. *Phys. Rev. Lett.*, 106:090502, Feb 2011.

[7] C. Gardiner and P. Zoller, editors. *Quantum Noise*, volume 1. Springer, 2 edition, 1998.

[8] H.J. Carmichael, editor. *Statistical Methods in Quantum Optics 1*, volume 1. Springer, 2 edition, 2002.

[9] A.G. Redfield. On the theory of relaxation process. *IBM Journal*, January 1957.

[10] Y. Wu and X. Yang. Strong-coupling theory of periodically driven two-level systems. *Phys. Rev. Lett.*, 98:013601, January 2007.

[11] F. Petruccione and H.P. Breuer, editors. *The Theory of Open Quantum Systems*. Oxford University Press, 2007.

[12] B. Kraus, H. P. Büchler, S. Diehl, A. Kantian, A. Micheli, and P. Zoller. Preparation of entangled states by quantum markov processes. *Phys. Rev. A*, 78:042307, October 2008.

[13] H.J. Carmichael, editor. *Statistical Methods in Quantum Optics 2*, volume 2. Springer, 2 edition, 2002.

[14] A. Wallraff, D. I. Schuster, A. Blais, L. Frunzio, R.-S. Huang, J. Majer, S. Kumar, S. M. Girvin, and R. J. Schoelkopf. Strong coupling of a single photon to a superconducting qubit using circuit quantum electrodynamics. *Nature*, 431(7005):162–167, 2004.

[15] A. Kamal, A. Roy, J. Clarke, and M. H. Devoret. Asymmetric frequency conversion in nonlinear systems driven by a biharmonic pump. *Phys. Rev. Lett.*, 113:247003, Dec 2014.

[16] A. Metelmann and A. A. Clerk. Nonreciprocal photon transmission and amplification via reservoir engineering. *Phys. Rev. X*, 5:021025, Jun 2015.

[17] A. Kamal and A. Metelmann. Minimal models for nonreciprocal amplification using biharmonic drives. *Phys. Rev. Applied*, 7:034031, Mar 2017.

[18] H. Pichler, T. Ramos, A.J. Daley, and P. Zoller. Quantum optics of chiral spin networks. *Phys. Rev. A*, 91:042116, April 2015.

[19] P.O. Guimond, H. Pichler, A. Rauschenbeutel, and P. Zoller. Chiral quantum optics with v-level atoms and coherent quantum feedback. *Phys. Rev. A*, 94:033829, September 2016.

[20] C. Müller, J. Combes, A. R. Hamann, A. Fedorov, and T. M. Stace. Nonreciprocal atomic scattering: A saturable, quantum yagi-uda antenna. *Phys. Rev. A*, 96:053817, November 2017.

[21] E. Doucet, F. Reiter, L. Ranzani, and A. Kamal. High-fidelity dissipative engineering using parametric interactions.

[22] P. Lodahl, S. Mahmoodian, S. Stobbe, P. Schneeweiss, J. Volz, A. Rauschenbeutel, H. Pichler, and P. Zoller. Chiral quantum optics. *Nature Review*, 541:473–480, January 2017.

[23] K. Stannigel, P. Rabl, and P Zoller. Driven-dissipative preparation of entangled states in cascaded quantum-optical networks. *New J. Phys.*, 14:063014, June 2012.

[24] I. Yang. Entanglement timescale. *Phys. Rev. D*, 97:066008, March 2018.